Transportation Research Part A 156 (2022) 113–132

Contents lists available at ScienceDirect

Transportation Research Part A

journal homepage: www.elsevier.com/locate/tra

Optimal pricing and investment in a multi-modal city — Introducing a macroscopic network design problem based on the MFD

Allister Loder [a,b,*], Michiel C.J. Bliemer [c], Kay W. Axhausen [b]

[a] Chair of Traffic Engineering and Control, Department of Mobility Systems Engineering, School for Engineering and Design, TU Munich, Munich, Germany

[b] Institute for Transport Planning and Systems, ETH Zurich, Switzerland

[c] Institute of Transport and Logistics Studies, University of Sydney, Australia

ARTICLE INFO

Keywords:
Pricing
Investment
MFD
Congestion
Bus
MPEC

ABSTRACT

Improving the performance of an existing transportation system is a challenge for engineers and policy makers as many dimensions and system design variables are interacting. In this paper, we propose the three-dimensional macroscopic fundamental diagram network design problem (3D-MFD-NDP). It is a strategic macroscopic tool to identify the directions of decision making in a multimodal transportation system, where the provision of roads and public transport services are interacting with costs for cars and public transport services in the performance of the entire road surface transportation system. The 3D-MFD-NDP models their effects aggregated at the network level and does not locate all measures to the road network. The objective function of the introduced 3D-MFD-NDP is minimizing the total travel time, while the design variables of the problem are the user costs for cars and bus tickets, the bus headway, the share of dedicated bus lanes and the length of the road network. The advantage of the 3D-MFD-NDP compared to existing approaches is that it is formulated as a mathematical program with equilibrium constraints (MPEC) that allows a fast closed-form solution instead of being simulation-based, usually computing many details not required in strategic decision making. We apply the 3D-MFD-NDP to the greater area of Zurich to study two different problems. First, we investigate how the current network performance can be increased by pricing and investment measures. Despite difficulties in identifying reliable cost information for the provision of roads, we find that substantial travel time savings are possible, especially when limiting car use by restricting its space and increasing its costs. Second, we investigate the response to a 20% population growth in urban and suburban regions with car and public transport prices as well as bus frequency as the free design variables. We find that the system can accommodate the population growth, but as the system costs are shared among more users, the costs per trip are lessened, which attenuates the steering effect of prices.

1. Introduction

We build our transportation infrastructure for carrying people and goods. However, too many vehicles on the road at the same time leads to congestion, makes journey speeds unsatisfactory and increases negative external costs. At the same time, replacing cars with buses can benefit the overall flow of passengers. However, the optimal solution is not only having buses, as bus journeys

* Corresponding author at: Chair of Traffic Engineering and Control, Department of Mobility Systems Engineering, School for Engineering and Design, TU Munich, Munich, Germany.
E-mail address: allister.loder@tum.de (A. Loder).

https://doi.org/10.1016/j.tra.2021.11.026
Received 16 December 2020; Received in revised form 8 November 2021; Accepted 30 November 2021
Available online 7 January 2022

require users to walk to and from the stop and accept waiting time at a bus stop, which can extend travel times substantially. Therefore, how much traffic and which combination of buses and cars is optimal for a city and how should it be priced to cover the transportation system's costs and support the optimal behavioral response in mode choice? This question is key to transport planning and has been raised since the second half of the 20th century (Smeed, 1968).

This question relates to the trade-off of congestion externalities and human preferences for (not) sharing the vehicle, e.g. a bus or ride sharing. Consequently, this question aligns at least with four relevant strategic and tactical decision dimensions of urban transportation. Most notably, the question relates to the traditional network design problem (NDP), i.e. how network size and design affect congestion and travel choices (e.g. Boyce, 1984; Magnanti and Wong, 1984; Friesz, 1985; Migdalas, 1995; Yang and Bell, 1998), but also how a bus network should be designed and operated (e.g. Patz, 1925; Sonntag, 1977; Salzborn, 1972; Schéele, 1980; Holroyd, 1965; Ceder and Wilson, 1986; Guihaire and Hao, 2008; Kepaptsoglou and Karlaftis, 2009; Ibarra-Rojas et al., 2015). A further strategic decision is the allocation of dedicated infrastructure to certain modes, e.g. buses or high occupancy vehicles (e.g. Black et al., 1992; Currie et al., 2004; Menendez and Daganzo, 2007; Gonzales and Daganzo, 2012; Gonzales et al., 2010; Zheng and Geroliminis, 2013). Compared to the previously mentioned approaches on single modes, the literature on urban transportation NDPs focusing on combining or interacting some of the previously mentioned networks and modes is scarce (Miandoabchi et al., 2012; Farahani et al., 2013). Fourth and last, adequate or optimal pricing (note that we for simplicity subsume all relevant costs, e.g., public transport ticket costs, road pricing, car registration and fuel taxes, under the term pricing) for infrastructure use and mobility (e.g. Pigou, 1920; Small and Verhoef, 2007; Parry, 2009; Parry and Small, 2009; Anas and Lindsey, 2011; de Palma and Lindsey, 2011; Kraus, 2012; Tirachini and Hensher, 2012; Tirachini et al., 2014b,a), which has been frequently cited as a powerful tool to influence behavioral responses, but that is also required to cover the costs for road infrastructure and buses, eventually supported by an external subsidy.

Ultimately, for cities to understand how to optimize mobility, all four dimensions (road network design, bus network design and operations, dedicated lanes, and pricing) have to be combined. So far, methodological opportunities to do so seem to be missing as many NDPs are limited to some of the above dimensions or are applied to hypothetical networks. However, the macroscopic fundamental diagram (MFD) offers a novel opportunity to link the (multimodal) network topology physically consistent to the average network journey time when the network is loaded with demand (Daganzo and Geroliminis, 2008; Leclercq et al., 2014). As there exists now large-scale empirical evidence for the MFD (Geroliminis and Daganzo, 2008; Loder et al., 2019a), the MFD can be used for policy making. As the concept of the MFD is mode-abstract and applies to all vehicles in an urban road network, its extension to capture multimodal traffic is natural, most notably in the 3D-MFD for buses and cars (Geroliminis et al., 2014; Loder et al., 2017; Fu et al., 2020). Recently, Barmpounakis and Geroliminis (2020) conducted a field experiment in Athens where multimodal trajectories of all vehicles have been collected using a swarm of drones, i.e., ground truth data for an entire network. Such data allows to estimate multimodal MFDs at an unprecedented scale (Paipuri et al., 2021), which shows how multimodal MFDs can be estimated everywhere. First policy-relevant applications of the MFD and 3D-MFD are multimodal pricing (Geroliminis and Levinson, 2009; Zheng and Geroliminis, 2020), bus lane allocation (Zheng et al., 2017; Dantsuji et al., 2017) or integrated bus lane allocation and mobility pricing (Dantsuji et al., 2021). Furthermore, the 3D-MFD allows to investigate the impact of the bus network design (Dakic et al., 2021). Most of the infrastructure adaption applications are simulation-based approaches, as most likely no physically consistent functional form for the 3D-MFD exists which directly reflects the changes to the network topology. In this paper, we use a recently proposed functional form for the 3D-MFD that captures explicitly the physical properties of the network (Loder et al., 2019b). Consequently, this particular functional form for 3D-MFD requires no separate re-simulation anymore and physically meaningful speeds for each mode can be directly obtained from the vehicle accumulations of both modes and macroscopic network topology and its associated changes.

Therefore, we combine this functional form with strategic, tactical and pricing decisions of urban spatial and transport planning and introduce as a new fundamental concept the 3D-MFD-Network Design Problem (3D-MFD-NDP), formulated as a mathematical problem with equilibrium constraints (MPEC). The MFD is also flexible to model details of traffic where needed and abstract everything else into a trip factory, making urban scale modeling much simpler (Daganzo, 2007). Consequently, the 3D-MFD-NDP is a novel application in long-term transportation system analysis planning and design to analyze strategies for multi-modal urban mobility at large urban scale.

The 3D-MFD-NDP can be formulated as a bi-level optimization problem. At the upper level, multi-modal mobility assets (transport infrastructure and public transport vehicles) and pricing decisions are made according to an objective function describing a mobility goal, e.g., minimize total travel time in the network, and at the lower level passenger flows and traffic distributes across routes and modes following Wardrop's equilibrium principle in a static traffic assignment. Thus, we formulate the 3D-MFD-NDP as a mathematical program with equilibrium constraints (MPEC) (Luo et al., 1996), where we formulate the equilibrium constraints as a mixed complementarity problem (MCP), following Rutherford (1995), Nagurney (1993) and van Nieuwkoop (2014). Additional capacity and economic constraints ensure physically and politically meaningful solutions. In other words, the 3D-MFD-NDP is a single optimization problem where the multi-modal interactions and dependencies of infrastructure investments, pricing decisions and behavioral responses are jointly analyzed. In this paper, we focus on the core mechanisms of the 3D-MFD-NDP for the policy analysis. This includes describing the morning commute into the city, one of the most demanding times for the urban transportation system. The pricing design variables are then the costs for public transport tickets (season ticket) and car registration and fuel taxes. As we use for the 3D-MFD the functional form proposed by Loder et al. (2019b), (possible) network design variables of the city's mobility assets are road network length, bus service frequency and share of dedicated bus lanes. However, as the 3D-MFD-NDP is a concept that can be enriched with more details where needed, it may be further extended. Other functional forms for the multi-modal MFD with physically meaningful parameters and thus design variables can be used too. For example, Loder et al. (2021) proposed

a (mathematically more complex) 4D-MFD for a combination of bicycle, bus, and car with physically meaningful parameters (and thus design variables).

In this paper, we apply the proposed 3D-MFD-NDP to study investment and pricing policies that may improve the morning commute in the greater Zurich region in Switzerland. In a multi-modal city like Zurich, we focus on the city's mobility assets of road infrastructure and public transport. For Zurich, we study two different problems. First, improving the current situation (2018) under various strategies when the government subsidy is reduced to zero: (i) using the current road infrastructure and (dis)-investment in buses, (ii) allowing for road infrastructure (dis)-investment and buses, (iii) allowing (dis)-investment in both mobility assets and reducing parking capacity by 30% in the city. Second, investigating whether the transportation system is able to accommodate the expected 20% population growth in the greater Zurich region and how pricing can support an optimal outcome.

This paper is organized as follows. In Section 2 we introduce the mathematical formulation of the 3D-MFD-NDP and discuss each constraint. In Section 3 we explain how the 3D-MFD-NDP is implemented in a case study. Then, in Section 4 we investigate optimal investment and pricing strategies for greater Zurich using the 3D-MFD-NDP. Last, we summarize our findings and conclude the paper in Section 5.

2. Model

We would like to point out that our network design problem aims to redesign an existing transport system instead of generating an entirely new transport system. This means that an existing transport system serves as input into the model as a starting point and that a redesigned system can be thought of as modifications to the number of lanes on roads (instead of changing the road structure) or in the frequency of public transport (instead of changing public transport routes).

Our network design problem considers trips in a regional area during the morning commute where the travel demand and network topology are given and fixed. The transport system offers a set of $\mathcal{M}$ transport modes with two elements, $m \in \{\text{bus}; \text{car}\}$. Define mobility tools $t \in \mathcal{T} = \{\text{car}; \text{abo}; \text{both}\}$, where residents can have a car, a public transport season ticket (abo),[1] or both.

In the following, we discuss the 3D-MFD-NDP elements sequentially. First, we define the input variables in Section 2.1. Second, we introduce the design variables and the objective function in Section 2.2. Then we provide the set of equilibrium constraints in Section 2.3, the physical capacity constraints in Section 2.4, and the economic constraints in Section 2.5. Thereafter, we formulate the entire 3D-MFD-NDP in Section 2.7. Table 1 lists all the sets used in this model and Table 2 summarizes all variables and parameters used in this model. Note that we use the $\perp$ symbol to indicate complementarity between an equation and the associated variable.

2.1. Input variables

To distinguish input variables from other variables, we denote all input (i.e., the network's current situation and the model's benchmark) variables with an overline. Let $\overline{\pi}_t^{\text{fix}}$ and $\overline{\pi}_m^{\text{var}}$ denote the current fixed (e.g. annual car tax or public transport discount card) and variable costs (e.g. fuel excise tax or fare per kilometer) per unit distance associated with mobility tool t and mode m, and let $\overline{c}^{road}$ and $\overline{c}^{bus}$ be the unit price per kilometer road infrastructure and price per bus, respectively. Let $\overline{S}$ denote the current transport subsidy.

From a spatial perspective for MFD-based applications, the network is partitioned into small and homogeneously congested traffic zones k (Ji and Geroliminis, 2012). Multiple zones allow to account for spatial heterogeneity in the allocation of space, e.g. comparatively more dedicated space to buses in the CBD compared to other zones. Consequently, the region is divided into several small MFD zones or reservoirs as shown in Fig. 1, where each zone k has internal flows and exchanging flows. Each zone k has the following characteristics: current total length of the road infrastructure $\overline{L}_k$, total number of parking spots $\overline{P}_k$, current total length of bus infrastructure $\overline{B}_k$, current total bus passenger capacity $\overline{Z}_k$, current average bus service headway $\overline{H}_k$, share of $\overline{L}_k$ dedicated to buses $\overline{\eta}_k$, and the design commercial speed of buses $\overline{V}_{c,\text{bus}}$. Note that in addition, the fundamental diagrams of buses and cars are inputs (see Loder et al. (2019b) for details).

The travel demand is given by the number of morning commuting trips $\overline{n}_{ij}$ between each origin zone i and each destination zone j. The current market share for mobility tool t is given by $\overline{Q}_{ijt}$.

We adopt the regional path perspective for trips (Yildirimoglu and Geroliminis, 2014; Yildirimoglu et al., 2015; Batista et al., 2019), where travelers choose regional path r out of $\mathcal{R}$ paths for each origin–destination pair. Regional paths as shown in Fig. 1b do not correspond to a specific route matched to the road network, but describe the distribution of trip lengths for a certain origin–destination pair in a specific zone k (Batista and Leclercq, 2019). Assuming static assignment, we focus on the mean of this distribution. Each regional path r from i to j has a given mode specific mean trip length $\overline{d}_{ijmr}$, and a given share of the trip length in each zone k, $\overline{\theta}_{ijkmr}$.

Besides the inputs variables defined above, there are several behavioral and network specific calibration parameters that are required as input. These will be discussed in the relevant subsections below.

[1] Abo is the abbreviation of the German word Abonnement.

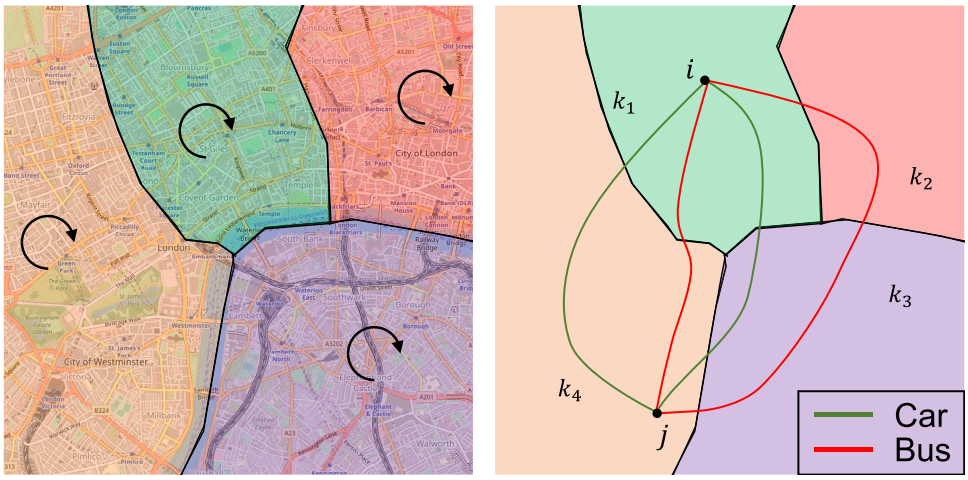

(a) Regional network (b) Regional paths

Fig. 1. Network idea for the MFD based traffic assignment. (**a**) illustrates the partition of an urban area into reservoirs with cars circulating in the reservoirs. Background map by OpenStreetMap contributors (**b**) shows the idea of regional paths across several regions.

Table 1
Model sets.

Index	Description
i, j, k	Zone identifier
m	Mode identifier with labels "*bus*" and "*car*"
r	Route identifier
t	Mobility tool portfolio with labels "*abo*", "*car*" and "*both*"

2.2. Design variables and objective function

In redesigning the transport system in our 3D-MFD-NDP, we optimize the following design variables: (i) network length L_k for each zone k, (ii) the share of dedicated bus lanes η_k for each zone k, (iii) the bus service headway H_k (which affects the frequency) for each zone k, (iv) the fixed cost π_t^{fix} of each mobility tool t, and (v) the variable cost π_m^{var} of each mode m.

We allow these design variables to vary within certain ranges (bounding boxes) around current levels $\overline{L}_k$, $\overline{H}_k$, $\overline{\eta}_k$, $\overline{\pi}_t^{\text{fix}}$ and $\overline{\pi}_m^{\text{var}}$. We assume that deviations from their current levels are sufficiently modest such that they do not change the network topology, i.e. we assume that mean trip lengths, $\overline{d}_{ijmr}$, and their share in each zone, $\overline{\theta}_{ijkmr}$, are exogenous.

The upper level objective y of the 3D-MFD-NDP is defined in Eq. (1) and corresponds to the total travel time of all travelers. Here, N_{ijmr} are the passenger flows between origin i, destination j, on mode m, using route r, and T_{ijmr} is the corresponding travel time for each passenger. To account for the waiting time of bus passengers, we add half of the bus headway H_i at the trip's departure location i to the travel time. The indicator δ_m^{bus} is used to apply the waiting time only to bus passengers by equal to one if mode m is bus and zero otherwise.

$$y = \sum_{ijmr} N_{ijmr} \left(T_{ijmr} + \frac{H_i}{2} \delta_m^{\text{bus}} \right) \tag{1}$$

The costs for mode use will be accounted for in the income balance in Section 2.3. They are not accounted for in Eq. (1) for two main reasons. First, they have to be paid by travelers anyway to cover the infrastructure expenses. Second, this model does not include a mechanism for the travelers to generate income to reflect their trade-offs in time and money.

2.3. Equilibrium constraints

The 3D-MFD-NDP is a long-term oriented city-scale analysis method for multi-modal urban mobility. Thus, for the 3D-MFD-NDP we select a static traffic assignment to derive a closed-form strategic policy model, which does not require any sequential simulation of the dynamics of traffic, e.g. as done by Tilg et al. (2020) or Zheng et al. (2017). Using the 3D-MFD in such a way keeps the model simple for long-term policy questions, while maintaining physical consistency in the derivation of multimodal travel times in the static assignment. Nevertheless, additional complexity can be added to the model if required by explicitly modeling the dynamics in a sequential optimization routine, e.g., building on Yildirimoglu and Geroliminis (2014) or Mariotte et al. (2017).

Therefore, we adopt a static traffic equilibrium based on the 3D-MFD, formulated as a stochastic user equilibrium (SUE) following Wardrop's first principle of the user equilibrium based on perceived travel cost. We assume that travelers choose mode m and route

Table 2
Model variables and parameters.

Variable type	Symbol	Description
Design variables	L_k	Infrastructure length in zone k
	H_k	Bus service headway in zone k
	η_k	Share of dedicated bus lanes in zone k
	π_t^{fix}	Fixed price/tax component of mobility tool t
	π_m^{var}	Variable price/tax component of mode m
Intermediate variable	A_{km}	Accumulation of vehicles of mode m in zone k
	C_{ijmr}	Total path cost for travelers from zone i to zone j using mode m on route r
	$\check{C}_{ijmr}$	Total perceived path cost for travelers from zone i to zone j using mode m on route r
	c_k^{bus}	Unit costs for a bus in zone k
	c_k^{road}	Unit costs for roads in zone k
	F_{ijtm}	Fraction of using mode m with tool t between i and j
	M_{ij}	Minimum path cost from i to j
	N_{ijmr}	Flow of passengers from i to j using mode m and route r
	O	Total operational costs of the transportation system
	Q_{ijt}	Shares of mobility tool ownership between i and j
	T_{ijmr}	Total travel times for N_{ijmr}
	u_{ijt}	Utility for ownership of tool t between i and j
	V_{km}	Speed of mode m in zone k
	Z_k	Total bus passenger capacity in k
	π_{ijt}^{total}	Total cost of tool t between i and j
	ρ_i^B	Shadow price of bus capacity in zone i
	ρ_i^C	Shadow price of car ownership in zone i
	ρ_i^P	Shadow price of parking supply in zone i
	ρ_i^T	Shadow price of season ticket ownership in zone i
Parameter	$\overline{B}_k$	Length of bus infrastructure in zone k
	$\overline{z}_k$	Bus line overlapping factor in zone k
	$\overline{\alpha}_k$	Bus network design in zone k
	$\overline{\varepsilon}^{\text{bus}}$	Economies of scale of buses
	$\overline{\varepsilon}^{\text{road}}$	Economies of scale of road infrastructure
	$\overline{\mu}^R$	Scale parameter of route and mode choice
	$\overline{\mu}^M$	Price elasticity of mobility tool ownership
	$\overline{\varphi}_{ij}$	Unobserved preferences to use the bus from i to j

r with the lowest perceived costs, $\check{C}_{ijmr}$. Thus, a particular route and mode between origin i and destination j is only chosen if its perceived path costs MC_{ij} along that route are equal to the minimum path costs, i.e. $M_{ij} \equiv \min_{mr} \check{C}_{ijmr}$. In other words, $N_{ijmr} > 0$ only if its path costs are equal to the minimum cost M_{ij}. If costs exceed M_{ij}, the route is not used, i.e. $N_{ijmr} = 0$. This feature is captured in the complementary condition of Eq. (2).

$$\check{C}_{ijmr} - M_{ij} \geq 0 \quad \perp \quad N_{ijmr} \geq 0 \tag{2}$$

The perceived paths costs are defined according to Eq. (3), where C_{ijmr} are the actual path costs as defined by Eq. (4) and $\overline{\mu}_R$ is the associated scale parameter. This behavioral parameter requires calibration. Note that Eq. (3) is adopted from Chen (1999) and describes a simultaneous route and mode choice multinomial logit model. Usually, a nested logit is used to account for differences in error variance or a cross-nested logit is used to account for overlap in the choice alternatives (Vrtic, 2003). However, for the regional path formulation as suggested in this problem, no data is available to determine the order and scale parameter of nests. Therefore, for simplicity a multinomial formulation, assuming the same error variance for mode and route choice, is favored, but which is clearly a limitation of the proposed model formulation.

$$\check{C}_{ijmr} = C_{ijmr} + \frac{1}{\mu^R} \log\left(N_{ijmr}\right) \tag{3}$$

The path costs C_{ijmr} are the generalized cost of travel and combine as given by Eq. (4) the in-vehicle travel time T_{ijmr} for both modes and shadow prices resulting from the capacity constraints, i.e. for parking ρ^P, car ownership ρ^C, bus passenger capacity ρ^B, and season ticket ownership ρ^T. The associated constraints are introduced in Section 2.4. Note that the monetary costs for using a particular mode and mobility tools are separately considered in the mobility tool ownership constraints in Section 2.6. Further, the path costs contain for buses a general waiting time defined as half the headway H_i in departure zone i. Preferences of commuters and other factors that influence the choice as well are captured in $\overline{\varphi}_{ij}$ that requires calibration from data. See Section 3.3 for details

on the calibration.

$$C_{ij,\text{car},r} = T_{ij,\text{car},r} + \rho_i^C + \rho_j^P$$
$$C_{ij,\text{bus},r} = T_{ij,\text{bus},r} + \frac{H_i}{2} + \rho_i^B + \rho_i^T + \overline{\varphi}_{ij} \tag{4}$$

Travel times T_{ijmr} are calculated using Eq. (5) as the sum of travel times within each region along each route r. Here, V_{km} is the journey speed of mode m in sub-region k, $\overline{\theta}_{ijkmr}$ is the share of trip distance $\overline{n}_{ij}\overline{d}_{ijmr}$ of a regional path inside region k. Note that $\overline{\theta}_{ijkmr}$ is zero for all zones not crossed by a regional path. For buses, the travel time contains the in-vehicle time including dwelling behavior.

$$T_{ijmr} = \sum_k \overline{\theta}_{ijkmr} \frac{\overline{d}_{ijmr}}{V_{km}} \tag{5}$$

We derive the journey speeds from the 3D-MFD (Geroliminis et al., 2014; Loder et al., 2019b). The 3D-MFD is a network performance function that provides travel times in a network given the current demand. The shape of the 3D-MFD results from the features and the topology of the road and bus networks. Consequently, when changing the network design variables of the 3D-MFD-NDP, the 3D-MFD will change shape and size, affecting the speeds of both modes in a region and consequently affecting travel choices. In particular, the 3D-MFD links the current accumulation of cars, $A_{k,car}$, and buses, $A_{k,bus}$, as well as the total network length, L_k, the length of bus infrastructure, B_k, and the share of L_k that is dedicated to buses, η_k, to the average speed of mode m in region k as formulated by Eq. (6). The shape of the 3D-MFD results from the features and topology of the road and bus networks. Consequently, when changing the network design variables of the 3D-MFD-NDP, the 3D-MFD will change and thus affect the speeds in the network. The long-term oriented and urban-scale 3D-MFD-NDP focuses on the main mechanisms of multi-modal congestion in cities to obtain the average expected journey times for car and public transport users in the network. If more realism of urban traffic should be needed, Eq. (6) can accommodate this based on the smoothing of the observed traffic to the theoretical lower envelope (Loder et al., 2019b).

$$V_{km} = \text{3D-MFD}_{km}\left(A_{k,car}, A_{k,bus}, L_k, B_k, \eta_k\right) \tag{6}$$

In our traffic assignment model, we cannot use Edie's (1963) definition to calculate the accumulation or density as there is no evolution of time that would allow us to determine the exact coordinates of each vehicle in time and space, which means that we cannot clearly attribute the contribution of each single vehicle to a reservoir's accumulation. Therefore, we calculate each modes' vehicle accumulation differently. For the accumulation of cars, $A_{k,\text{car}}$, we assume a vehicle occupancy of one passenger to obtain the accumulation by Eq. (7). In this static traffic assignment, the flows along regional paths are the only source of information on the spatial distribution of vehicles moving from i to j. Thus, we approximate for a reservoir k the contribution of vehicles by their share of trip distance inside k. Later, we calibrate the model on observed speeds to ensure that the observed accumulation from Eq. (7) results in the observed speeds. Consequently, the validity of this link reduces with distance to the observed state.

$$A_{k,\text{car}} = \sum_{ijr} \overline{\theta}_{ijk,\text{car},r} N_{ij,\text{car},r} \tag{7}$$

We derive the accumulation of buses, $A_{k,\text{bus}}$, from the bus service headways H_k and the structure and design of the bus network (adopted from Daganzo (2010)) as given by Eq. (8). Note that the bus headway H_k is not only affecting the accumulation of buses in the network and thus the congestion mechanism (see Eq. (6)), but also the waiting time of bus travelers and thus path costs (see Eq. (4)). Regarding the bus network design, $\overline{\alpha}_k$ is an exogenous parameter describing the design of the bus network in each region for which $0 < \overline{\alpha}_k \leq 1$ holds. Close to its lower bound, $\overline{\alpha}_k$ describes a hub-and-spoke network, while at its upper bound it describes a grid network. Values in between are hybrid networks where one can see $\overline{\alpha}_k$ as the fraction of network exhibiting a grid network. As in many cities bus lines are partially overlapping, we introduce $\overline{z}_k$ that quantifies how many bus lines are overlapping on the bus infrastructure $\overline{B}_k$. In case no bus lines are overlapping, $\overline{z}_k = 1$, if two bus lines are overlapping on the entire network, then $\overline{z}_k = 2$ and so on. The values of parameters $\overline{z}_k$ and $\overline{\alpha}_k$ must be calculated from observations in complex (real) bus network designs with overlapping bus routes and hybrid network layouts. Last, $\overline{V}_{c,\text{bus}}$ is the design commercial speed of buses in the network. Note that Eq. (8) means that the accumulation of buses is insensitive to variation in the car accumulation and only a function of the design variable headway, i.e., only describing free-flow condition, no bus bunching cases and exact time-table following. Consequently, Eq. (8)'s validity decreases with the network-wide increase of such situations.

$$A_{k,\text{bus}} = \overline{z}_k \frac{2\overline{B}_k}{H_k} \frac{3\overline{\alpha}_k - \overline{\alpha}_k^2}{1 + \overline{\alpha}_k^2} / \overline{V}_{c,\text{bus}} \tag{8}$$

Lastly, Eq. (9) then provides the conservation of passenger flows for each origin and destination pair. The total travel demand $\overline{n}_{ij}$ between i and j has always to equal the total flow of passengers N_{ijmr} using all modes and routes between i and j. M_{ij} is the associated complementary variable. Importantly, as we are formulating the 3D-MFD-NDP based on regional paths, there is no requirement to explicitly model the in- and outflows at each node as in a link based assignment.

$$\overline{n}_{ij} - \sum_{mr} N_{ijmr} = 0 \quad \perp \quad M_{ij} \geq 0 \tag{9}$$

2.4. Physical system (capacity) constraints

The static traffic assignment model has a set of four inequalities that describe the physical constraints of the system and which have associated shadow price variables that factor into the path costs. The first constraint describes the parking supply in each zone as given by Eq. (10). Consequently, the total arrival car passenger flow cannot exceed the parking supply. If the parking demand exceeds the parking supply, then a non-zero shadow price, ρ_j^P, will ensure that the number of arriving cars is restricted to the parking supply. Note that the parking supply $\overline{P}$ in each zone is considered to be invariant against changes to the infrastructure length L, as much of it usually takes place in off-street parking facilities and curb-side parking only in residential roads.

$$\overline{P}_j - \sum_{ir} N_{ij,\text{car},r} \geq 0 \quad \perp \quad \rho_j^P \geq 0 \tag{10}$$

The second and third inequality captures the model's property that all departing trips of a zone of a certain mode must not exceed the availability of mobility tools in that zone. In other words, the number of car trips starting in i cannot be greater than the number of available cars in i as given by Eq. (11). Similarly, the number of outbound bus passenger trips cannot exceed the number of public transport season-tickets, or in brief *abos*, in that zone as formulated in Eq. (12). In these equations, Q_{ijt} describe the shares of mobility tool ownership, where the elements of set t are having only a car, an abo or having both. The calculation of Q_{ijt} is discussed in Section 2.6 and depends on current mobility tool ownership levels $\overline{Q}_{ijt}$ and the changes in total prices π_{ijt}^{total}. When the inequality becomes binding, the respective shadow prices ρ_i^C and ρ_i^T become non-zero.

$$\sum_j \left(Q_{ij,\text{car}} + Q_{ij,\text{both}}\right) \overline{n}_{ij} - \sum_{jr} N_{ij,\text{car},r} \geq 0 \quad \perp \quad \rho_i^C \geq 0 \tag{11}$$

$$\sum_j \left(Q_{ij,\text{abo}} + Q_{ij,\text{both}}\right) \overline{n}_{ij} - \sum_{jr} N_{ij,\text{bus},r} \geq 0 \quad \perp \quad \rho_i^T \geq 0 \tag{12}$$

The fourth inequality describes that the passenger capacity of the bus system is limited to a total passenger accumulation of Z_k as formulated in Eq. (13). The total bus passenger flows have to be always less or equal to that capacity. When supply equals demand, public transport users experience additional waiting time ρ_k^B in their departing zone as all arriving buses are full.

$$Z_k - \sum_{ijr} \overline{\theta}_{ijk,\text{bus},r} N_{ij,\text{bus},r} \geq 0 \quad \perp \quad \rho_k^B \geq 0 \tag{13}$$

The total bus passenger capacity in each region according to Eq. (14), where $\bar{A}_{k,bus}$ denotes the current accumulation of buses in region k and is a calibration parameter.

$$Z_k = \overline{Z}_k \frac{A_{k,\text{bus}}}{\overline{A}_{k,\text{bus}}} \tag{14}$$

2.5. Economic constraints

This set of constraints restricts solutions to the 3D-MFD-NDP where the revenue from mobility (ownership π_t^{fix} and use π_m^{var}) and the subsidy $\overline{S}$ equals the operational costs O for the city's mobility assets. This operational costs O for the city's mobility assets, i.e. the costs for the provision of roads and bus operations, are calculated with Eq. (15). Here, c_k^{road} and c_k^{bus} are the unit prices for the provision of infrastructure and buses, respectively, and may be higher or lower than current costs $\overline{c}_k^{\text{road}}$ and $\overline{c}_k^{\text{bus}}$ as explained later in this section. Consequently, the totals then depend on the size of the network L_k and number of buses $A_{k,\text{bus}}$.

$$O = \sum_k c_k^{bus} A_{k,\text{bus}} + c_k^{road} L_k \tag{15}$$

Then, the income balance of costs, revenue and subsidy is mathematically expressed in Eq. (16). Here, we assume that the total revenue counts towards the available budget for infrastructure spending, although in reality this is too simplistic as public funding and budgets are usually more complex (see our discussion in the calibration of the model in Section 4.1).

$$\sum_{ijt} \pi_t^{\text{fix}} \overline{n}_{ij} Q_{ijt} + \sum_{ijmr} \pi_m^{\text{var}} N_{ijmr} \overline{d}_{ijmr} + \overline{S} = O \tag{16}$$

The costs for buses c_k^{bus} and roads c_k^{road} can be subject to (dis-) economies of scale. Therefore, we account for this by the formulations for both costs in Eqs. (17) and (18), respectively.

These cost functions are calibrated using elasticity parameters $\overline{\varepsilon}_k^{\text{road}}$ and $\overline{\varepsilon}_k^{\text{bus}}$, where a negative value indicates economies of scale, a positive value indicates diseconomies of scale, and a zero value indicates constant costs.

$$c_k^{road}\left(L_k\right) = \overline{c}^{road} \exp\left(\overline{\varepsilon}_k^{\text{road}} \log\left(L_k / \overline{L}_k\right)\right) \tag{17}$$

$$c_k^{bus}\left(A_{\text{bus},k}\right) = \overline{c}^{bus} \exp\left(\overline{\varepsilon}_k^{\text{bus}} \log\left(A_{\text{bus},k} / \overline{A}_{\text{bus},k}\right)\right) \tag{18}$$

2.6. Mobility tool ownership constraints

The shares of mobility tool ownership Q_{ijt} depend on the current shares of ownership $\overline{Q}_{ijt}$ and the changes in total cost of ownership π_{ijt}^{total}. The total costs combine the fix costs or price of mobility tool portfolio t, π_t^{fix}, and the variable and distance-depending price of mode m, π_m^{var}, between i and j. Note that the term pricing and cost refers here only to those price components that are or can be imposed by the transport system operators, i.e., they do not include private costs. As commuters have choices of different routes and modes, when having both mobility tools, we calculate π_{ijt}^{total} as the average cost of all alternatives as defined in Eq. (19). Here, F_{ijtm} gives the fraction of using mode m with mobility tool set t (defined below in Eq. (20)) and the last term in parentheses gives simply the average trip distance.

$$\pi_{ijt}^{\text{total}} = \pi_t^{\text{fix}} + \sum_m \pi_m^{\text{var}} F_{ijtm} \left(\sum_r \frac{\overline{d}_{ijmr}}{|\mathcal{R}|} \right) \tag{19}$$

The fraction F_{ijtm} using mode m with mobility tool set t is defined according to Eq. (20). I_{tm} is an indicator function that equals one if t = abo $\wp$ m = bus or t = car $\wp$ m = car, and equals zero otherwise. In other words, when owning only either an abo or a car, only the respective mode can be used, i.e. $F_{ijtm} \equiv 1$, and the other mode cannot be used, i.e. $F_{ijtm} \equiv 0$. Only when having both mobility tools, F_{ijtm} can be different from zero or one as shown in Eq. (20). Then, F_{ijtm} is simply the number of mode m commuters over all commuters for each origin–destination pair having both mobility tools.

$$F_{ijtm} = \begin{cases} \dfrac{\sum_r N_{ijmr} - \overline{n}_{ij} \sum_{t'} I_{t'm} Q_{ijt'}}{\overline{Q}_{ijt}\, \overline{n}_{ij}}, & \text{if } t = \text{both} \\ I_{tm}, & \text{otherwise} \end{cases} \tag{20}$$

We then define the current total cost of ownership $\overline{\pi}_{ijt}^{\text{total}}$ using Eqs. (19) and (20) based on current prices $\overline{\pi}_t^{\text{fix}}$ and $\overline{\pi}_m^{\text{var}}$. The share of mobility tool ownership Q_{ijt} then deviates from its current share $\overline{Q}_{ijt}$ if π_{ijt}^{total} deviates from $\overline{\pi}_{ijt}^{\text{total}}$; the higher the price of tool t, the lower its share.

In this model, we reduce the complexity of choices for mobility tools typically available to individuals, as shown, for example, in Switzerland (Becker et al., 2017; Loder and Axhausen, 2018), to the three most prominent choices: only a car, only an abo, i.e. bus season-ticket, or both.

We model this relationship using a two-level logit model. We require two levels as choices are not independent. Thus, the first level considers whether individuals have both mobility tools or not; if not, the second level determines whether they have a car or abo. For the logit model, we then define the required utility functions as given in Eq. (21). The alternative specific constant (ASC) is related to the calibrated market share $\overline{Q}_{ijt}$. Utility changes with changes of total costs π_{ijt}^{total} relative to the current costs $\overline{\pi}_{ijt}^{\text{total}}$ with scale parameter $\overline{\mu}^M$ capturing the price elasticity of mobility tool ownership. Note that $\overline{\mu}^M$ is a behavioral parameter that requires calibration.

$$\begin{aligned} u_{ij,\text{both}} &= \log\left(\overline{Q}_{ij,\text{both}}\right) + \left(\pi_{ij,\text{both}}^{\text{total}} / \overline{\pi}_{ij,\text{both}}^{\text{total}} - 1\right) / \overline{\mu}^M \\ u_{ij,\text{not both}} &= \log\left(1 - \overline{Q}_{ij,\text{both}}\right) \\ u_{ij,\text{car}} &= \log\left(\overline{Q}_{ij,\text{car}}\right) + \left(\pi_{ij,\text{car}}^{\text{total}} / \overline{\pi}_{ij,\text{car}}^{\text{total}} - 1\right) / \overline{\mu}^M \\ u_{ij,\text{abo}} &= \log\left(\overline{Q}_{ij,\text{abo}}\right) + \left(\pi_{ij,\text{abo}}^{\text{total}} / \overline{\pi}_{ij,\text{abo}}^{\text{total}} - 1\right) / \overline{\mu}^M \end{aligned} \tag{21}$$

We then obtain the shares of mobility tool ownership $\overline{Q}_{ijt}$ using Eq. (22). Note that the formulation of a logit model ensures that the shares always add up to one.

$$\begin{aligned} Q_{ij,\text{both}} &= \frac{\exp\left(u_{ij,\text{both}}\right)}{\exp\left(u_{ij,\text{both}}\right) + \exp\left(u_{ij,\text{not both}}\right)} \\ Q_{ij,\text{car}} &= \left(1 - Q_{ij,\text{both}}\right) \frac{\exp\left(u_{ij,\text{car}}\right)}{\exp\left(u_{ij,\text{abo}}\right) + \exp\left(u_{ij,\text{car}}\right)} \\ Q_{ij,\text{abo}} &= \left(1 - Q_{ij,\text{both}}\right) \frac{\exp\left(u_{ij,\text{abo}}\right)}{\exp\left(u_{ij,\text{abo}}\right) + \exp\left(u_{ij,\text{car}}\right)} \end{aligned} \tag{22}$$

2.7. Problem formulation

The 3D-MFD-NDP is then defined in Eq. (23) with objective function y defined in Eq. (1) and the constraints defined in Eqs. (2)–(22): The 3D-MFD-NDP is looking for the solution of the network design and pricing variables that reduces the total system travel

time, subject to the constraints that the existing demand is assigned to the network, that the physical capacity constraints are satisfied and that monetary expenditures equal revenue.

$$\begin{aligned} &\text{minimize} && y \\ &\text{subject to} && (2)\text{–}(9) && \text{solving MCP} \\ &\text{and} && (10)\text{–}(14) && \text{solving capacity constraints} \\ &\text{and} && (20)\text{–}(22) && \text{solving ownership constraints} \\ &\text{and} && (15)\text{–}(19) && \text{solving economic constraints} \end{aligned} \tag{23}$$

The problem formulated in Eq. (23) is highly non-linear and non-convex, making solving the problem for optimality difficult. This applies to every network design problem formulated as an MPEC or a bi-level optimization problem, specifically as they are NP hard (Colson et al., 2007). Thus, even for the simplest networks solving for global optimality is challenging (Sarvi et al., 2016), but advances in global optimization algorithms for NDPs (Luathep et al., 2011; Wang et al., 2013) provide opportunities for further development of the 3D-MFD-NDP. This paper does not aim to make a contribution with respect to solving NDPs, but adopts existing algorithms that find a locally optimal (and possibly global) solution that demonstrates the potential of improving the network design and services. Specifically, to solve the problem, we use the MPEC command within GAMS (General Algebraic Modeling System) with the NLPEC solver. Note the limitations, however, that the GAMS manual mentions that this model type is still under development, namely "The state-of-the-art for MPEC solvers is not nearly as advanced as that for other model types" and that robustness issues and limitations by problem size should be expected (GAMS Development Corporation, 2018). Therefore, advances in solving MPECs will improve the applicability of the proposed 3D-MFD-NDP, but they could also alter the results presented in Section 4 of the paper.

2.8. Practical limitations

These technical limitations have practical implications. Just providing spatial demand information is quite unlikely to solve for the global optimal network configuration for this demand. Contrary, the model aims to inform decision makers about how the current situation can be improved by adopting pricing and investment measures. Therefore, the model requires a sensitive calibration to the current situation, physically meaningful definition of the bounding box for the design variables and setting the starting values for each variable to the current situation. This applies to the equilibrium constraints and complementary variables, as with holding the design variables at current calibration values, the solver should re-compute the current situation immediately. Attention should also be paid to the price parameters of buses and road infrastructure as their choice immediately defines the feasible solutions as governed by Eq. (16). We experienced that with improper calibration, starting values and bounding boxes, the problem becomes infeasible. As we find later in the price sensitivity analysis, small variations in these parameters can impact substantially the resulting solutions and thus alter the model's implications.

Nevertheless, when the problem formulated in Eq. (23) faces a substantial increase in travel demand, the simultaneous formulation of mode and route choice ensures that travel speeds are not driven to gridlock with zero speeds, but travelers are rather allocated from the slower car mode to the then faster public transport mode until equilibrium is reached. As there is usually some dedicated infrastructure for buses, the network average speed will approach zero, but stay positive, avoiding infeasible or unacceptable solutions. However, the latter is a theoretical worst case as additional public transport passenger capacity is endogenously provided in the 3D-MFD-NDP to make up for the passenger increase.

2.9. Policy limitations

As with every equilibrium (transport) model, the validity of model results is the strongest around its calibration point. Thus, any optimal solutions that is found distant to the calibration point should be scrutinized. For example, the MFD assignment model will be calibrated to speeds in Section 3 as the resulting travel times are a key input to travel behavior decisions, by reducing the network length to obtain the observed speeds. Then, when modeling other scenarios than the morning peak, the speed calibration point might become inaccurate and may lead to suboptimal policy implications. In addition, the current model is formulated for a central European transportation system structure, where it is typical for many commuters to have a car and season ticket. Thus, other regional contexts may have to alter some constraints to fit to their specific context to obtain valid policy implications. This also holds for the definition and parameters of Eq. (16) as mentioned above in a policy context. Further, the 3D-MFD-NDP discusses average network effects of policy measures but cannot represent the effects of local link-based measures. Importantly, as the 3D-MFD-NDP requires an a-priori definition of zones, the model outcomes may be sensitive to a specific zone selection. Consequently, the 3D-MFD-NDP can give investment and pricing directions for policy making, but not recommendations for their specific localization. Lastly, the model is formulated for a morning commute that might be representative for long-term planning in some regions, in others it may not with increasing share of the elderly and more leisure activities taking place.

3. Model implementation

The empirical implementation of the model, i.e., Eq. (23), requires adoption to typical empirical settings such as having a city design with a substantial inflow of commuters from outside of the city (discussed in Section 3.1), identifying suitable zones for the MFD (discussed in Section 3.2) and calibration of the model parameters (discussed in Section 3.3).

3.1. City design

The typical commuting layout of cities is that work places are aggregated at urban centers and employees live in suburban areas. While many urban centers also provide residential areas, suburban areas do not exhibit a substantial amount of workplaces. Thus, suburban areas are commuting trip origins, but not destinations, while the trips' destinations are located in the urban centers. Ignoring these commuting trips would miss a substantial load to the transportation system in the city. Therefore, the 3D-MFD-NDP does not only focus on the multi-modal transportation system inside the city, but also accounts for inbound trips from suburban areas outside of the city. Note that this is a simplification of the model in Section 2 where all zones are origins and destinations.

The model can account for this by adding trip origins outside of the city and connect them with regional paths to each zone in the city. To capture directional effects from everywhere around the city, it is recommended to add trip origins in at least every cardinal direction. Those living close to each trip origin outside the city is then aggregated into the respective trip origin. The travel times of inbound commuters combine the travel time to the city boundary and then the travel time inside the city. While the travel time inside the city follows Eq. (5), the travel time outside the city must not necessarily follow the MFD, but can also follow the Bureau of Public Roads function or any other meaningful relationship.

3.2. Zoning

The mathematical problem requires a spatial aggregation as the model is macroscopic and the MFD exists for neighborhoods or larger parts of a city. MFDs are typically estimated for neighborhoods that cover less than 10 km^2 (Geroliminis and Daganzo, 2008). These neighborhoods should have a redundant network (route alternatives), homogeneous network with similar streets and link fundamental diagrams insensitive to turning movements (Daganzo and Geroliminis, 2008) as well as being homogeneously loaded (Sun et al., 2014). In other words, cities are divided into several reservoirs or zones as shown in Fig. 1a where traffic traverses from zone to other zones as seen in Fig. 1b on similar urban streets. These zones are obtained by partitioning methods (e.g., Ji and Geroliminis, 2012; Ambühl et al., 2019), but which are usually intended to incorporate network dynamics that do not exist for the 3D-MFD-NDP as proposed here.

3.3. Calibration

The 3D-MFD-NDP requires calibration to an observed point, most notably the behavioral parameters $\overline{n}_{ij}$, $\overline{Q}_{ijt}$, $\overline{\varphi}_{ij}$, $\overline{\mu}^{M}$, $\overline{\mu}^{R}$, $\overline{\varepsilon}^{\text{bus}}$ and $\overline{\varepsilon}^{\text{road}}$ as well as the network specific parameters $\overline{z}_k$ and $\overline{\alpha}_k$. The information on the origin and destination matrix $\overline{n}_{ij}$ as well as shares of mobility tool ownership for origin and destination pairs $\overline{Q}_{ijt}$ are usually available from travel surveys or from census information. The behavioral elasticities $\overline{\mu}^{R}$ and $\overline{\mu}^{M}$ can also be derived from travel surveys. $\overline{\varphi}_{ij}$, the unobserved preferences for using a certain mode between origin and destination can be obtained from observed modal splits between the respective origin and destination. Its value is obtained by solving for each origin and destination pair a nonlinear programming problem of minimizing the squared difference between the observed mode share and resulting mode choice from Eq. (9).

Further, the 3D-MFD-NDP requires calibration and estimation of the pricing variables and parameters, e.g., $\overline{\pi}_t^{\text{fix}}$, $\overline{\pi}_m^{\text{var}}$, $\overline{c}_k^{\text{bus}}$, $\overline{c}_k^{\text{road}}$, $\overline{\varepsilon}^{\text{bus}}$, $\overline{\varepsilon}^{\text{road}}$, and $\overline{S}$. Intuitively, the values should reflect the current situation. However, it is quite unlikely that with all parameters known, the income balance from Eq. (16) will hold. Therefore, we suggest that the subsidy $\overline{S}$ should be adjusted in order to make the income balance hold in the calibration.

Last, the 3D-MFD-NDP also requires calibration and estimation of the infrastructure parameters and variables of the 3D-MFD and the network assignment. The 3D-MFD calibration values for $\overline{L}_k$, $\overline{B}_k$ and $\overline{\alpha}_k$ can be estimated directly from OpenStreetMap, while H_k and η_k require information from bus agency, e.g., H_k can be derived from time tables and η_k can be derived from maps usually available within agencies. The bus line overlap $\overline{z}_k$ can be obtained by solving Eq. (8) for $\overline{z}_k$ in the calibration point. The parking capacity $\overline{P}_k$ can be either obtained from a census or if not available, by adding all car arrivals in zone k corrected by the estimated parking spot vacancy in peak hour. Contrary, the network assignment variables, namely vehicle accumulation and speed, require empirical observations for calibration. These observations are usually available from the city's road traffic agency and the public transport agency. As it is quite unlikely that for the given 3D-MFD and the demand matrix $\overline{n}_{ij}$ will one obtain perfectly the observed vehicle accumulations and speeds. We suggest to slightly reduce the infrastructure length $\overline{L}_k$ until the gap between the predicted and observed speeds is close to zero. This procedure is intuitive as due to directional traffic, not all roads are similarly used and some lanes are rarely used compared to others. Removing these from the 3D-MFD adds thus more realism to the modeled scenario.

4. Policy analysis

We apply the 3D-MFD-NDP to the morning commute in the greater region of Zurich, Switzerland to study optimal transport pricing and investment strategies. Section 4.1 discusses the model preparation for this specific Zurich analysis, where Table 3 summarizes the economic and behavioral parameters used for the model calibration. We solve the MPEC formulated in Eq. (23) for two different problem sets. First, in Section 4.2 we optimize in various infrastructure and pricing scenarios the current (2018) situation. Second, we study the response of the transportation system to a 20% growth.

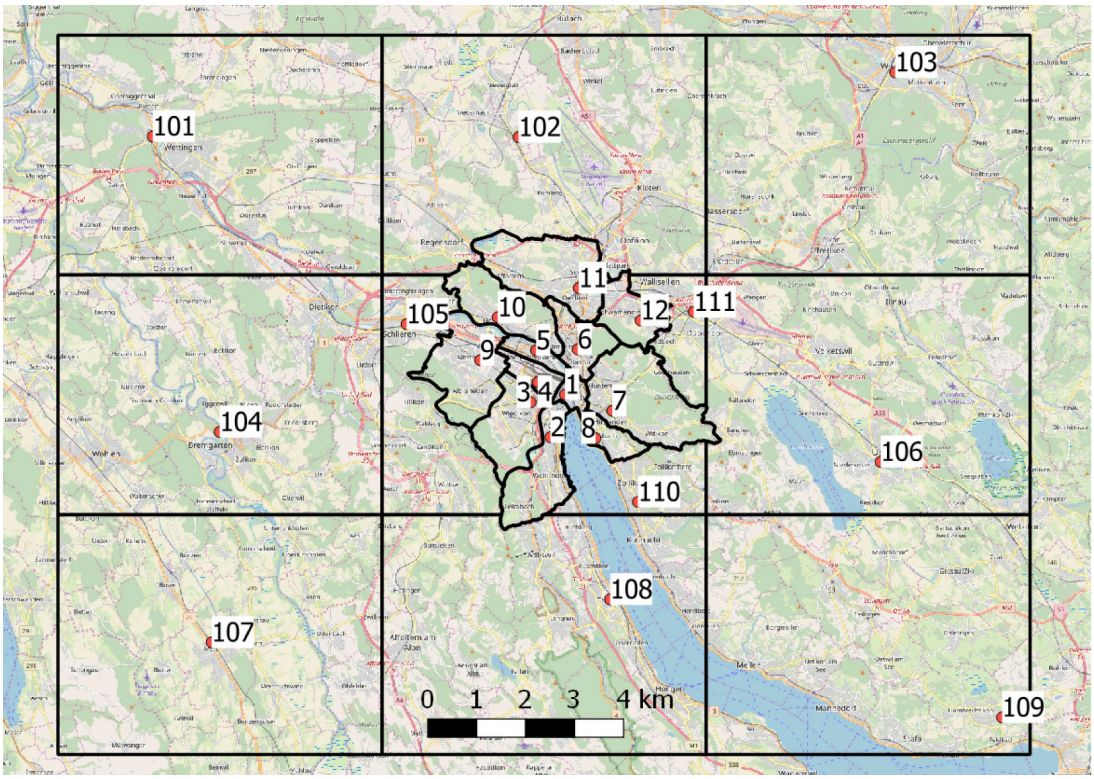

Fig. 2. Zonal system for the case study. Background map by OpenStreetMap contributors.

4.1. Model preparation

Fig. 2 shows the extent of the case study area. Zones 1–12 denote the city where the commuters live and work and zones 101–111 correspond the suburban residential areas mentioned in Section 3.1. Zones 1–12 each exhibit a 3D-MFD as formulated by Loder et al. (2019b) to obtain the speeds as given in Eq. (6). The speeds for zones 101–111 are considered to be fixed to typical morning commute journey speeds.

The zoning for this case study follows the city of Zurich district's boundaries. In total, there are 12 districts ("Kreise") which all are less than 10 km^2 in size, but have well connected road networks. This zoning is chosen in order to map unambiguously the available commuting matrix. With the present zoning, no highway or similar roads are available for internal trips. Further removing all residential streets from the network for the MFD leaves a homogeneous and well connected network with main urban streets. The zones' centroids correspond to the origin and destination of trips, i.e., where the demand is aggregated, are derived from each district's geometric centroid.

For the origin and destination matrix $\overline{n}_{ij}$ we use the commuting matrix of a synthetic Swiss population for the agent-based simulation MATSim (Bösch et al., 2016). We re-scale the total arrivals in each of the twelve inner zones of MATSim's commuter matrix to correspond to the work place totals used by the national transport model (NPVM). From the 2015 Swiss travel survey we obtained the mode shares of outbound trips of each region (Swiss Federal Statistical Office and Swiss Federal Office for Spatial Development, 2017).

We obtained spatial information on the regional paths for both modes from the Google directions API: For each origin and destination pair, we requested the shortest route including alternative routes without using the motorway and calculated $\overline{\theta}_{ijkmr}$ thereof. We calibrated the 3D-MFD speed functions based on OpenStreetMap data and measurements based on the data used by Loder et al. (2017). One of the key features of Zurich's transport system is that the headway is identical for almost all services in the city. Arguably, this is easy to memorize for all travelers and the resulting short connection time ensures that journeys can be done without planning, i.e., looking up the journey in advance. Therefore, we do not consider a zone-specific headway H_k, but a fixed headway H for the entire city. Nevertheless, the question can be asked whether zone-specific headways would improve the objective function further.

In this model formulation, the term pricing refers only to the price components that are or can be imposed by the transport system operators and do not include the private costs of vehicle ownership. For Zurich, we consider the following mobility tool portfolio and pricing situation. When having a car, commuters face fix costs as well as variable costs per unit distance. In particular, for the fixed car price component, in the following defined as *Car tax*, this covers, e.g., the annual car registration tax and parking costs at

Table 3
Price and cost information for the calibrated 3D-MFD-NDP.

Parameter or observed value	Unit	Value
$\bar{c}^{bus}$	(CHF/day bus)[a]	3100
$\bar{c}^{road}$	(CHF/day km)[b]	1900
$\bar{\epsilon}^{bus}$	(–)[g]	$\{0; -0.2\}$
$\bar{\epsilon}^{road}$	(–)	$\{0; 0.2\}$
$\bar{\pi}^{\text{fix}}_{abo}$	(CHF/day)[c]	3
$\bar{\pi}^{\text{var}}_{abo}$	(CHF/km)[d]	0
$\bar{\pi}^{\text{fix}}_{car}$	(CHF/day)[e]	5
$\bar{\pi}^{\text{var}}_{car}$	(CHF/km)[f]	0.1
$\bar{\mu}^{R}$	(–)	10
$\bar{\mu}^{M}$	(–)[h]	−0.5

[a]This cost includes the capital costs and all costs required to operate a bus fleet (overhead, maintenance, bus stops, cleaning etc.). It is obtained by dividing the total annual cost of Zurich's bus operator VBZ by the number of buses and trams in their fleet, and then transform this figure to a daily figure. For this study, we used data from 2016.

[b]The cost for roads is obtained from the bureau of statistics that publishes the annual expenditures for construction, operation, maintenance and planning of the city's entire urban road network (highways are not included as they are operated by the federal government). This figure most likely does not include full capital costs. https://opendata.swiss/de/dataset/statistik-der-schweizer-stadte-strassenrechnung.

[c]Costs for annual ZVV pass (season-ticket) for three zones approx CHF 1200, divided by 365 days.

[d]Set to zero as we focus on the option of season-tickets.

[e]Assuming fix annual taxes, fees etc. of CHF 800, and annual parking costs of CHF 1.200, in total CHF 2.000, divided by 365 days.

[f]For urban traffic, assuming 8 liter per 100 km, a fuel price of CHF 1.30 per liter.

[g]Bösch et al. (2017) reported for car fleet operators economies of scale of around 20% in Switzerland. As data for bus operators in Switzerland is not available and this section aims to show applicability of the model, the value for car fleets is transferred to bus fleets for simplicity.

[h]Average fuel price elasticity estimated by Erath and Axhausen (2010).

the destination. As in Zurich the only variable car price component is the fuel tax (and its associated taxes), we denote the variable car price component as *Fuel tax*. However, this tax is charged by distance and is thus insensitive to vehicle propulsion technology. When having a bus season-ticket (or as defined here "*abo*"), commuters face only fix costs, but no variable costs, denoted as *Ticket costs* in the following. In other words, it is not possible to purchase single ride or distance-dependent season tickets. This situation reflects the situation in Switzerland where most public transport commuters own a season-ticket. When having both mobility tools, commuters have to pay the costs of both. We obtain from the 2015 Swiss travel survey the shares of mobility tool ownership $\overline{Q}_{ijt}$ based on all commuters living in the case study zones. Note that we assign all commuters without a car or "*abo*" (season-ticket) to the "*abo*" category. For most origin–destination pairs, this share was less than ten percent of the total origin–destination demand.

In Table 4 we summarize the calibrated model's most relevant performance indicators. For the situation in Zurich as shown in Fig. 2 it is important to explain how the mobility tool revenue relates to the public budget. We define for inbound commuters that they only pay a fraction of their mobility tool expenses to the city's transport budget. The fraction is determined by the fraction of their trip length in the city. We further define that 60% of the ticket revenue goes to the budget, while we consider the remaining part is going to the railway operators (not considered in this analysis) and to the cantonal transport agency. Similarly, we assume for the car that only 25% of the revenue is directed to the city's budget, while the remaining revenue goes to private companies (e.g. petrol stations) and other tax purposes (e.g. the CO_2 tax).

Lastly, we have to calibrate or define meaningful upper and lower bounds for all design variables. Arguably, the model is calibrated to the current situation and solutions far off this situation, e.g. building twice as many roads, are physically not feasible. Therefore, we allow only for changes in the length of the road network of ±10 % of its length. We further limit the length of dedicated bus infrastructure to 90% of the actual network length of buses because some interactions with cars, e.g. at intersections are unavoidable. For the prices, we set the following upper values $\pi^{\text{fix}}_{abo} = 20$ (CHF/day), $\pi^{\text{fix}}_{car} = 50$ (CHF/day), and $\pi^{\text{var}}_{car} = 1$ (CHF/km). We further bound the number of bus services with a headway between 1 and 12 min.

4.2. Optimization of current situation

We study the optimization for three infrastructure measures under the directive of reducing the exogenous subsidy $\overline{S}$ to zero: First, we analyze the opportunities to reduce travel time based on the current road infrastructure, i.e., we fix $L_k = \overline{L}_k$ for all zones k. Second, we allow for (dis)-investment in road infrastructure, i.e., allowing L_k to vary within the set bounding box. Third, we reduce parking supply, $\overline{P}$, by 30% in the city and having all design variables free. For each scenario, we analyze three pricing alternatives: *all free*, *fixed ticket* and *fixed car*. The alternative *all free* has the season ticket costs and the car taxes (fixed and variable) as free

Table 4
Transport network calibration values for the 3D-MFD-NDP.

Observed value	Unit	Value
$\sum \overline{L}$	(km)	1400[a]
$\sum \overline{A}_{\text{bus}}$	(bus)	1040[b]
$\overline{H}$	(h)	0.125
$\overline{S}$	(CHF/day)	48'000[c]
Share of car trips	(–)	0.33[d]
$\overline{Q}_{\text{car}}$	(–)	0.18
$\overline{Q}_{\text{both}}$	(–)	0.35
$\overline{Q}_{\text{abo}}$	(–)	0.47

[a]Includes the city's and the canton's road network, the infrastructure of public transport and the space on the high capacity roads. The calibration of the 3D-MFD to observed speeds, L is overestimated by around 200 km.
[b]This vehicle number is twice as much as the bus operator owns, but this results from the problem that we cut bus routes at the zones from Fig. 2 and consequently count vehicles several times.
[c]Calculated as the difference between infrastructure costs and revenue from mobility tools.
[d]Calculated based on travel kilometers.

variable, while the other two alternatives discuss the effects when season ticket costs or car taxes should not change compared to the current situation.

We study the model's sensitivity by varying the prices of the city's mobility assets (road infrastructure and buses) by ±10% and considering economies of scale at the calibration price levels of roads and buses. Importantly, when increasing the price of buses by 10%, called *high bus price*, we decrease the price for road infrastructure by 10%. Contrary, when decreasing the price of buses by 10%, called *low bus price*, we increase the price for road infrastructure by 10%.

Importantly, the 3D-MFD-NDP offers a variety of possibilities for scenario runs and sensitivity analyzes, but as this paper aims to illustrate applicability and feasibility, we outline the main mechanisms in the following to show the model's features at the global and local level.

4.2.1. Global results

In Fig. 3 we show the results compared to the calibration point of the model. Thus, all listed changes are relative. Across all scenarios it can be seen that the objective of reducing travel time can be achieved by more than 10% even at a small decrease in system cost. This shift can only be achieved by incentivizing to use the bus instead of the car and to reduce car ownership. Allowing for (dis)-investment decreases the objective function further, while no substantial differences can be observed between the second and third scenario when imposing the parking restrictions. Arguably, the behavioral shift is caused by pricing and taxes and not by limiting parking (see Section 4.2.2 for discussing the shadow price of parking).

When comparing the pricing alternatives, the *all free* alternative is reducing travel time the most as it increases the fuel tax substantially, discouraging car ownership and travel. Contrary, when fixing the season ticket costs, reduction in car ownership and use can only be achieved by increasing the car registration tax and reducing the fuel tax to the minimum (lower bound). However, when allowing for (dis)-investment in road infrastructure and when considering economies of scale of roads and buses as well as lower bus prices, the reduction of the fuel tax becomes less or even positive.

Interestingly, the calibration prices for buses seem to be that high that to compensate for the reduced subsidy it is more favorable for travel time reduction to decrease the number of buses than to increase season ticket costs and car taxes. Only when considering economies of scale for buses or lower bus costs, buses become more affordable for reducing the total travel time at the available income.

Further, it can be seen that in every scenario the 3D-MFD-NDP suggests that the total travel time can be reduced by allocating more space to public transport. Note that we set the upper limit for dedicated bus lanes to an 80% increase compared to the calibration point. In the scenarios that allow for (dis)-investment in road infrastructure (see Fig. 3**c–f**), it can be seen that for most scenarios the road network length is reduced. Only at higher bus prices and lower road costs, expanding the road network becomes more likely.

4.2.2. Local results

As the 3D-MFD-NDP acts not only on a global but also on a local scale, this section discusses local effects inside the global results.

For this, we show in Fig. 4**a** the changes to the car speed (correlating with accessibility), in Fig. 4**b** the total travel production of cars (correlating with negative externalities), and in Fig. 4**c** the changes in network length in each city zone. We compare the calibration point to scenario runs where (dis)-investment in roads and buses is possible. Then we solve for each pricing alternative (*all free*, *fixed ticket* and *fixed car*) and then for reducing parking supply by 30% scenario. Last, in Fig. 4**d** we show the shadow price of parking ρ^P resulting from Eq. (10) for each zone when reducing parking supply by 30% and having either season ticket costs or car taxes fixed.

In Fig. 4**a** we see that in all scenarios, the speed in each zone and, thus, the accessibility is improved in some cases perhaps surprisingly quite substantially. Fig. 4**b** shows that in each zone the travel production is decreased, which emphasizes a reduction

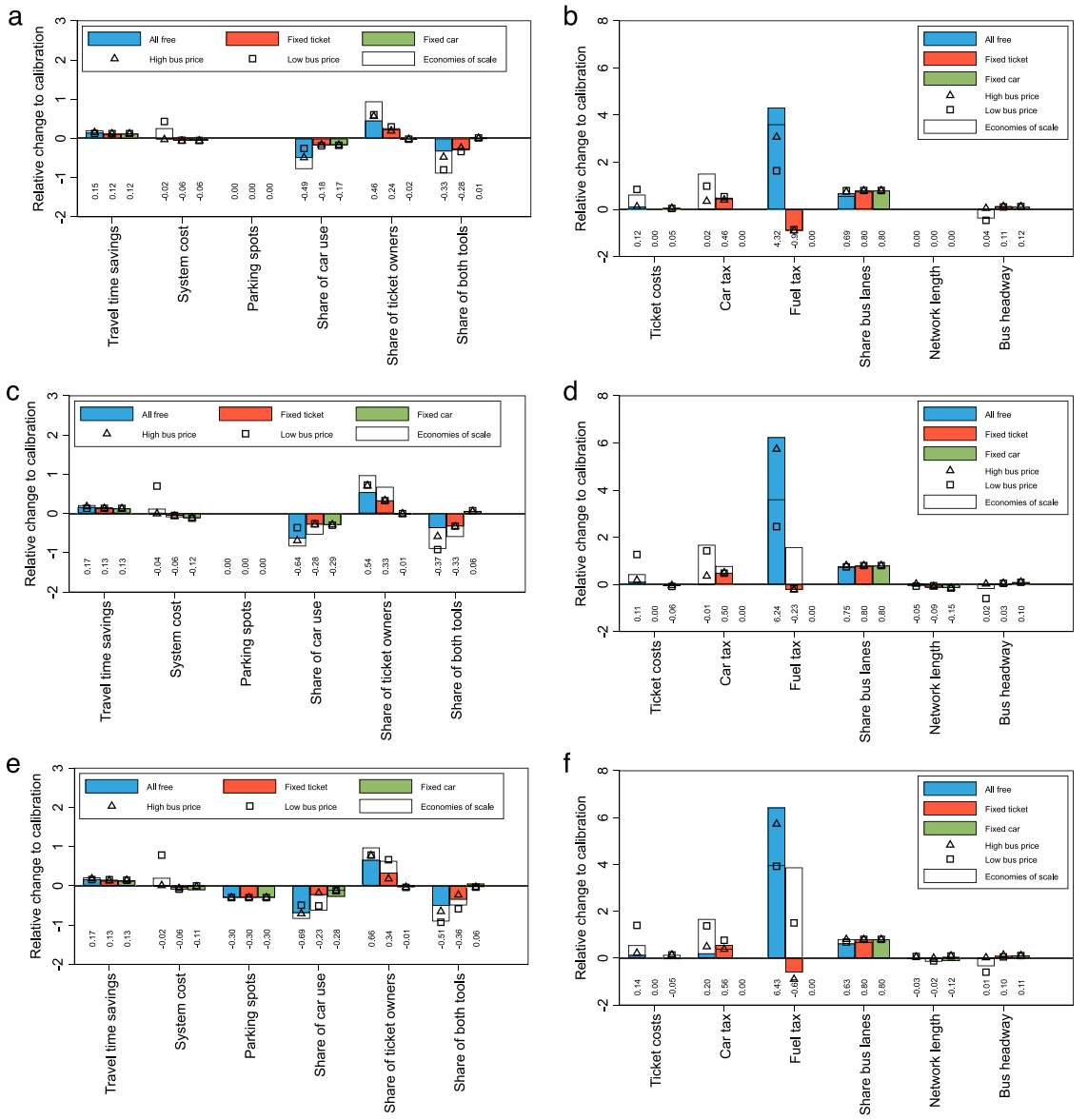

Fig. 3. Scenario results for the Zurich case study. The figures on the left show the most relevant system performance indicators and the figures on the right the changes to the 3D-MFD-NDP design variables. The numbers above the horizontal axis correspond to the value for the calibration bus and road prices without economies of scale. (**a–b**) shows the results for the optimization scenario for the current road infrastructure. (**c–d**) shows the results for the optimization scenario allowing for road infrastructure (dis)-investment. Panels (**e–f**) show the results for the optimization scenario with reducing parking supply by 30%.

in the negative externalities of traffic. Fig. 4**c** emphasizes that the resulting speeds result from changes in the travel production and (dis-) investment measures into the road infrastructure, which in all except for three cases suggest that a disinvestment is the best strategy. Although some of the measures shown in Fig. 3 are (politically) infeasible, the local effects shown here underline what improvements could be achieved. Fig. 4**d** shows the shadow price for parking supply is not non-zero in every zone. This means that the parking constraint is not binding everywhere and that in the zones with non-zero ρ^P, an implementation of (higher) parking prices at the calculated marginal cost would achieve the reported reduction in total system travel time. Note that the pricing alternative *all free* results in $\rho^P = 0$ for all zones because the shift of car drivers to buses is entirely achieved by making car driving unattractive by increasing car taxes. The occurrence of the most non-zero ρ^P values for the *fixed ticket* alternative is intuitive. In this particular alternative, the range of car taxes, compared to the fixed season ticket costs, is too small to incentivice car drivers to use public transport. Recall that mobility tool ownership results from the relationship between season ticket prices and car taxes. Thus, $\rho^P = 0$ is required to ensure that not more car drivers arrive than parking spots are available.

Lastly, to illustrate the system changes on the 3D-MFD and thus the entire network capacity, we compare in Fig. 5 the 3D-MFD shapes from district (Kreis) 1 and 11 as shown in Fig. 2 for two situations. First, the current - *calibrated* - situation and,

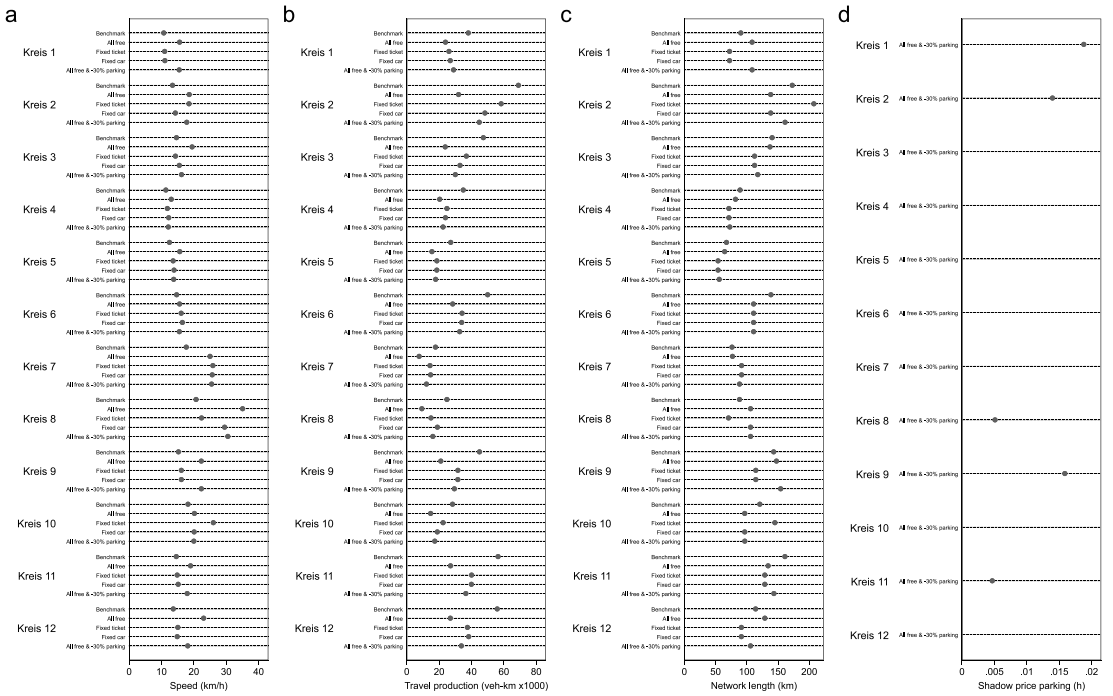

Fig. 4. Illustrating zonal results of the 3D-MFD-NDP. (**a**) shows the car speed changes in each zone. (**b**) shows the changes in car travel production in each zone. (**c**) shows the changes in the network length in each zone. (**d**) shows the shadow price of parking in each zone when reducing the parking supply.

second, the solution to the 3D-MFD-NDP where (dis)-investment in both mobility assets is possible at the calibration price levels (see Table 3) without economies of scale and the pricing alternative is *all free*. Note that the MFD shape follows from the design variables (infrastructure length and share of dedicated bus lanes) and that the 3D-MFD itself is not the objective function. Note that to compare all 3D-MFDs, they have the same scales. It can be clearly seen that Kreis 1 has a much smaller network than Kreis 11 and that in the solution, the share of infrastructure used by both modes is substantially reduced. However, regarding the length of the road network infrastructure the results are different. In Kreis 1, the solution suggests to increase the road network infrastructure to achieve an almost entirely dedicated public transport network and thus maintain the current space available for cars. Contrary, the solution suggests for Kreis 11, that the road network infrastructure is reduced and with more of that dedicated to public transport, the space available for cars is reduced.

4.3. Scenario population growth

We use the proposed 3D-MFD-NDP to study the impact of population growth on the multimodal urban transportation system in Zurich. The Canton of Zurich expects a population growth of 20% until 2040 compared to 2020 (Statistisches Amt des Kantons Zürich, 2021). In this analysis we discuss three cases of population growth: (i) even distribution of growth in all zones, (ii) concentration of new developments in the city of Zurich (zone numbers 1–12 in Fig. 2), (iii) settlement of new residents in suburban areas outside the city of Zurich (zone numbers > 100 in Fig. 2) to describe urban sprawl. All new residents attain the shares of mobility tool ownership and trip demands following the existing demand in each zone. For each case, we solve Eq. (23) first with all pricing and investment variables fixed to describe a *without policies*-scenario. Second, we let the public transport service headway, the public-transport season-ticket price and the variable car costs be free variables to describe a *with policy*-scenario. In other words, the first scenario can be seen as *business-as-usual*, while the latter is the optimized scenario.

Fig. 6 summarizes the results of this analysis. Fig. 6**a** intuitively shows that the objective function (total travel time) is growing with growing demand, while the overall increase is lowest in the concentration case where trips are shorter compared to the urban sprawl case. A substantial difference between the two scenarios cannot be seen, this is supported with the overall car travel production also showing in Fig. 6**b** only small differences between both scenarios. The increase in population means that most of the system costs are shared among more people as seen in Fig. 6**c**, which results in lower user costs per capita (Fig. 6**d**), i.e., eventually reducing the prices for season-tickets (Fig. 6**e**) and variable car costs (Fig. 6**f**). Note that the variable car costs are at their lower bound. The system cost savings per capita are larger in the urban sprawl case as more buses can removed from the system compared to the concentration case as seen in Fig. 6**g**. Arguably, in the concentration case, more bus capacity is required to carry commuters. Contrary, the individual savings in the user costs are larger in the concentration case compared to the urban sprawl case. Arguably, while suburban commuters still must pay variable car costs, urban residents with a higher share of season-ticket ownership save substantially on the fixed costs of season-tickets.

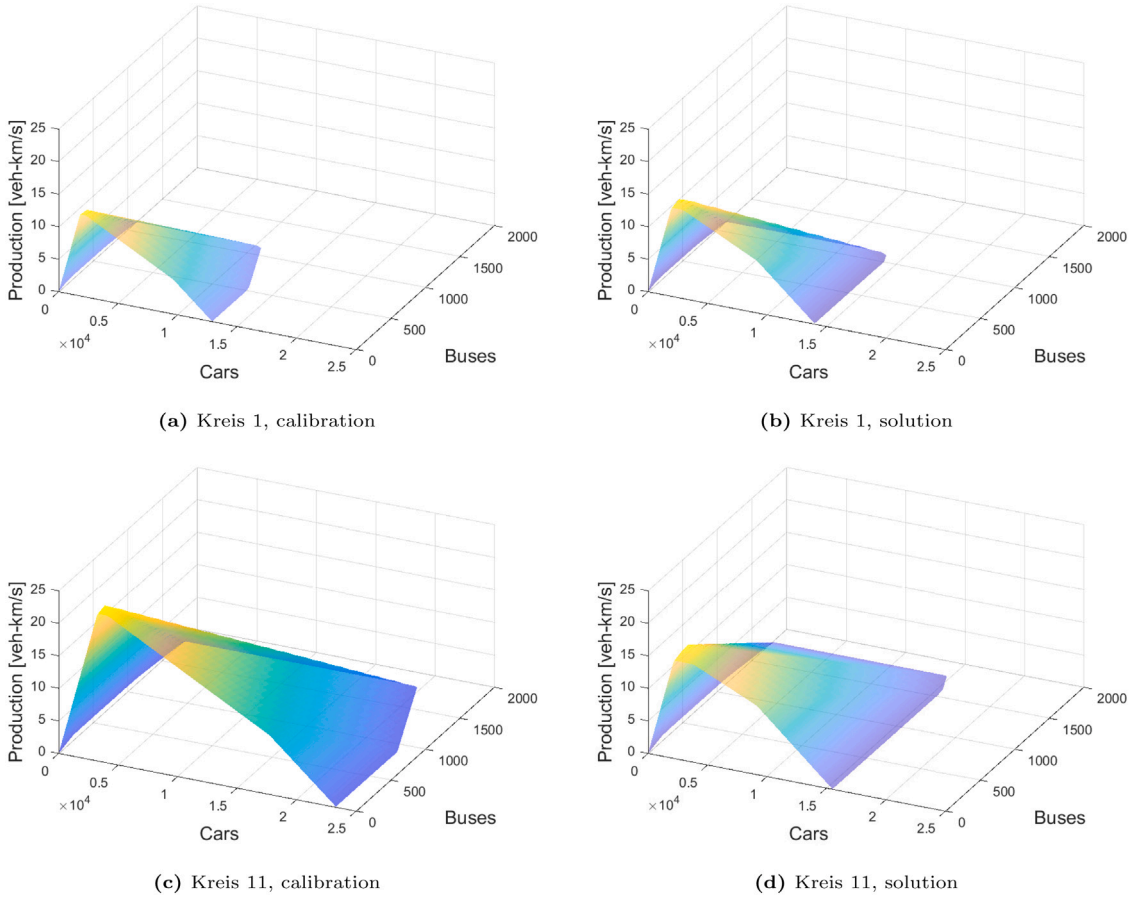

(a) Kreis 1, calibration

(b) Kreis 1, solution

(c) Kreis 11, calibration

(d) Kreis 11, solution

Fig. 5. Comparison of calibrated (left column) and the resulting (right column) 3D-MFDs for zone (Kreis) 1 and 11 of the 3D-MFD-NDP where (dis)-investment in both mobility assets is possible at the calibration price levels without economies of scale and the *all free* pricing alternative. The first row refers to Kreis 1 and the second column to Kreis 11. (**a**) calibrated 3D-MFD for Kreis 1. (**b**) solution 3D-MFD for Kreis 1. (**c**) calibrated 3D-MFD for Kreis 11. (**d**) solution 3D-MFD for Kreis 11.

As the prices for both mobility tools decreased in all scenarios, no unexpected drastic shift in mobility tool ownership can be observed. Car ownership changed from 17% in the current situation to 10% in the concentration case, 12% in the even distribution and 12% in the urban sprawl case. Season-tickets changed from 48% to 46% in the concentration case, 50% in the even distribution and 58% in the urban sprawl case. Having both mobility tools changed from 35% in the current situation to 44% in the concentration case, 38% in the even distribution and 30% in the urban sprawl case.

Last, the increased demand along with the savings lead to a reduction in network speeds as seen in Fig. 6**h**, where the impact is larger in the concentration case compared to the urban sprawl case as in the first case all interactions are consolidated in the central areas of the city. However, in the concentration case, more population is accessible in the city compared to the urban sprawl case, eventually leading to higher overall levels of population-weighted accessibility and its associated benefits (Hansen, 1959).

This analysis also shows some limitations of the proposed 3D-MFD-NDP in its present form. First, the common case in Europe to have several mobility tools leads to the situation that minor pricing adjustments affect mobility tool ownership in the first place, but not its impact on traffic. Thus, to establish a direct link between costs and mode use, having two mobility tools should be limited. Second, the variable car costs must not correspond to any externalities caused by traffic, but its value just follows the income balance of the mobility system. However, if required, congestion pricing could be added by using, e.g., the approach proposed by Zheng et al. (2012). Third, the results also underline the modeled complexity, where the limitations of current MPEC solvers mean that the existence of local minima can affect policy implications.

5. Conclusions

In this paper, we introduced the multi-modal macroscopic fundamental diagram network design problem (3D-MFD-NDP) formulated as a mathematical program with equilibrium constraints (MPEC), which is built around a recently introduced functional form for the 3D-MFD (Loder et al., 2019b). The 3D-MFD-NDP is looking for the solution of the network design and pricing variables

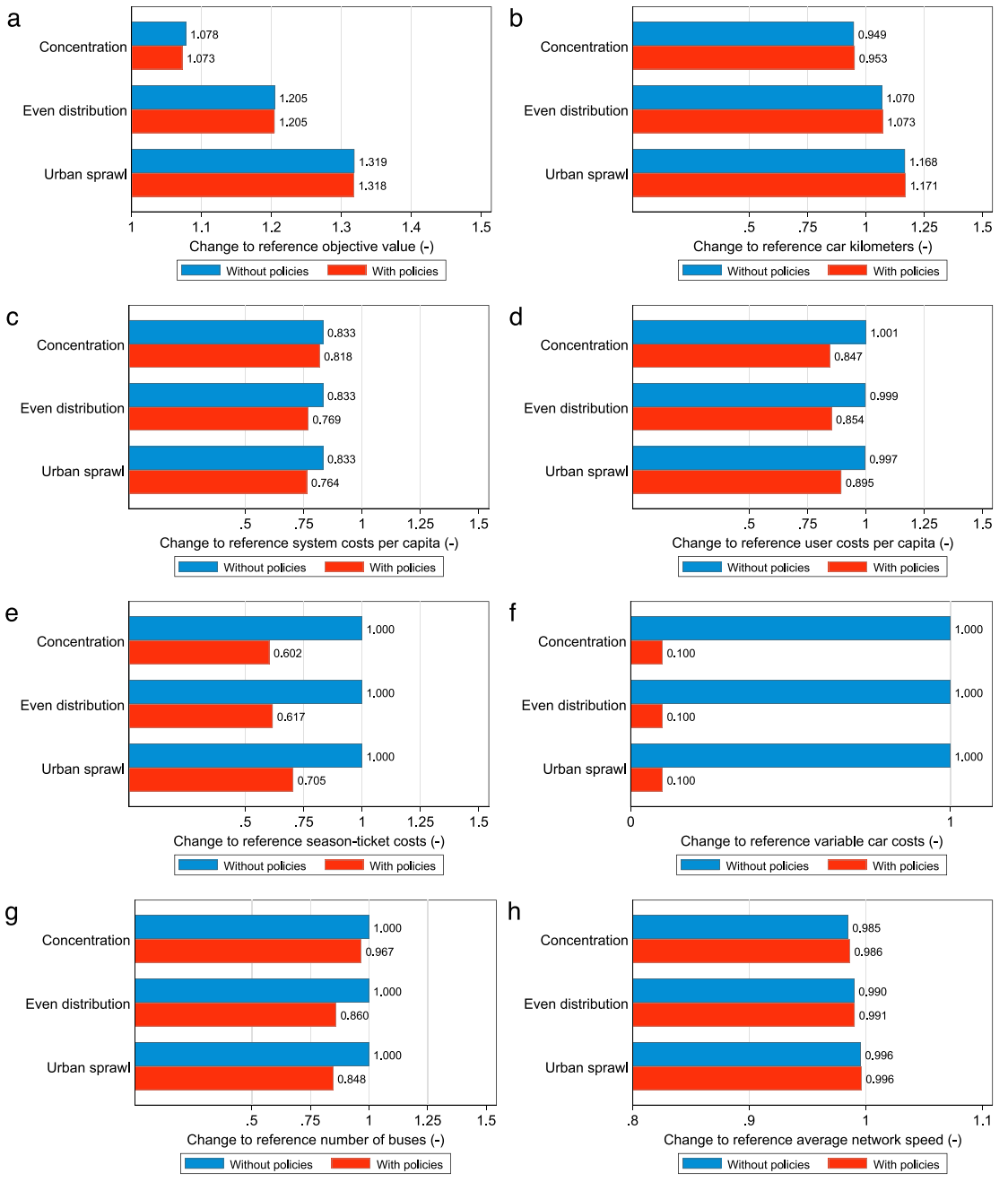

Fig. 6. Effects of a 20% population increase in the case study area. The population is distributed across zones either following a concentration in the urban area (zones 1–12), an even distribution across all zones, or following urban sprawl by settling in the zones around the urban area (zones > 100). In each of the three cases, the effects of growth are derived for the no policy case (blue) and when prices and the bus frequency as design variables can be adjusted (red). (For interpretation of the references to color in this figure legend, the reader is referred to the web version of this article.)

that behavioral response minimizes the total system costs of the urban transportation system, subject to the constraints that the existing demand is assigned to the network and then and that monetary expenditures equal revenue. The proposed 3D-MFD-NDP provides a macroscopic and multi-modal approach to combine road network design, bus network design and operations, allocation of dedicated lanes, and mobility pricing in a single optimization problem. The design variables of the proposed 3D-MFD-NDP formulation are road network length, bus service frequency, share of dedicated bus lanes, and the fixed and variable price components of cars and public transport that can be imposed by the transport system operators. We applied the 3D-MFD-NDP

to the greater Zurich region to study, first, how the current situation in the year 2018 can be improved by pricing and infrastructure investment measures and, second, how the transportation system responds to a 20% increase in population.

The 3D-MFD-NDP describes important and timeless conflicts and trade-offs in strategic transportation planning. Consequently, the results of increasing car and fuel taxes and improving public transport for a better system performance do not surprise. Nevertheless, the 3D-MFD-NDP helps to understand the direction and magnitude of changes required for an improved or even optimal performance. The formulated 3D-MFD-NDP focuses on key design variables for urban transportation and their interactions and thus support planners and decision makers to derive quantitative results. The proposed model corresponds to a fundamental concept that can be extended in future research in several ways to fulfill more specific requirements: (i) the objective function can also be cost-based, welfare-based or accessibility based to discuss other policy goals that go beyond travel times; (ii) demand can be elastic and is not limited to discuss only the morning commute; (iii) addressing distributional effects among the population; and (iv) refine transport modeling with advances in MFD modeling as discussed in the next paragraph. In addition, further advances in solving bi-level optimization problems and MPECs (e.g., Luathep et al., 2011; Wang et al., 2013) could contribute to a wider and more general application of the 3D-MFD-NDP.

Refining in future research the 3D-MFD-NDP's transport model also addresses its current limitations. First, we use a static traffic assignment for two reasons: (i) its simplicity has widely been used for long-term planning (ii) the functional form for the 3D-MFD describes its lower envelope (Loder et al., 2019b) and does not capture in its present formulation the dynamics of a network. Thus, using a dynamic traffic assignment would not only improve the model's power for policy making, but would also allow to include traffic control strategies (e.g. Haddad and Geroliminis, 2012) and the effects of transit priority (e.g. Guler and Menendez, 2014; Guler et al., 2016). Second, the 3D-MFD-NDP's solution strongly depends on the calibration of the transportation infrastructure and cost curves. Without reliable estimates, the solution space is not only wrongly defined but also provides inaccurate results and then in turn inappropriate policy implications. As these cost functions are usually hard to obtain – as it is the case for Zurich as well – the model requires a careful data preparation and calibration phase. Third, the topological design of the bus and road network as well as the effects of other modes, e.g. pedestrians, motorcycles and bicycles is not part of the optimization in this formulation of the 3D-MFD-NDP, because it is still ongoing research how these dimensions influence the shape of the MFD. Thus, once this knowledge is available, future research can re-formulate the 3D-MFD-NDP. Last, the current representation cannot account for the emergence of a Braess paradox when adding or removing links to the network, arguably as the influence of this paradox on the MFD (shape) is not yet well studied. Thus, prior to including this to our problem, this understanding has to be developed. Thus, accounting for these contributions in future research would improve the quantitative implications that the 3D-MFD-NDP provides.

In closing, the 3D-MFD-NDP presented here is a novel approach to bundle several important strategic urban and transport planning decisions into a single optimization problem based on the multi-modal MFD. The proposed 3D-MFD-NDP is simple and computationally fast as it does not requires separate traffic simulations, but it still accounts for many interactions and feedback of physical properties and behavioral responses. Thus, urban planners and policy makers can use the 3D-MFD-NDP to generate and compare various different policy scenarios subject to their city-specific constraints to identify the optimal investment pricing strategy for their city. As the objective is to minimize total system costs – the social optimum – the proposed 3D-MFD-NDP proves a macroscopic and multi-modal tool to derive strategies for mobility for everyone.

CRediT authorship contribution statement

Allister Loder: Conceptualization, Methodology, Software, Formal analysis, Data curation, Writing. **Michiel C.J. Bliemer:** Conceptualization, Investigation, Methodology, Supervision, Writing. **Kay W. Axhausen:** Conceptualization, Methodology, Supervision, Writing.

Acknowledgment

This work was supported by ETH Research Grant ETH-04 15-1. The authors wish to thank Renger van Nieuwkoop and Thomas F. Rutherford for helpful comments in the development of the model. The authors also wish to thank the anonymous referees for improving the paper through their comments.

References

Ambühl, L., Loder, A., Zheng, N., Axhausen, K.W., Menendez, M., 2019. Approximative network partitioning for MFDs from stationary sensor data. Transp. Res. Rec. 2673 (6), 94–103. http://dx.doi.org/10.1177/0361198119843264.

Anas, A., Lindsey, R., 2011. Reducing urban road transportation externalities: Road pricing in theory and in practice. Rev. Environ. Econ. Policy 5, 66–88. http://dx.doi.org/10.1093/reep/req019.

Barmpounakis, E., Geroliminis, N., 2020. On the new era of urban traffic monitoring with massive drone data: The pNEUMA large-scale field experiment. Transp. Res. C 111, 50–71.

Batista, S.F., Leclercq, L., 2019. Regional dynamic traffic assignment framework for macroscopic fundamental diagram multi-region models. Transp. Sci. http://dx.doi.org/10.1287/trsc.2019.0921.

Batista, S.F., Leclercq, L., Geroliminis, N., 2019. Estimation of regional trip length distributions for the calibration of the aggregated network traffic models. Transp. Res. B http://dx.doi.org/10.1016/j.trb.2019.02.009.

Becker, H., Loder, A., Schmid, B., Axhausen, K.W., 2017. Modeling car-sharing membership as a mobility tool: A multivariate probit approach with latent variables. Travel Behav. Soc. 8, 26–36. http://dx.doi.org/10.1016/j.tbs.2017.04.006.

Black, J., Lim, P., Kim, G., 1992. A traffic model for the optimal allocation of arterial road space: A case study of seoul's first experimental bus lane. Transp. Plan. Technol. 16 (3), 195–207. http://dx.doi.org/10.1080/03081069208717483.

Bösch, P.M., Becker, F., Becker, H., Axhausen, K.W., 2017. Cost-based analysis of autonomous mobility services. Transp. Policy 64, 76–91. http://dx.doi.org/10.1016/j.tranpol.2017.09.005.
Bösch, P.M., Müller, K., Ciari, F., 2016. The IVT 2015 baseline scenario. In: 16th Swiss Transport Research Conference. Ascona, http://dx.doi.org/10.3929/ethz-b-000117938.
Boyce, D.E., 1984. Urban transportation network-equilibrium and design models: Recent achievements and future prospects. Environ. Plan. A 16 (11), 1445–1474. http://dx.doi.org/10.1068/a161445.
Ceder, A., Wilson, N.H.M., 1986. Bus network design. Transp. Res. B 20 (4), 331–344. http://dx.doi.org/10.1016/0191-2615(86)90047-0.
Chen, H.-K., 1999. Dynamic Travel Choice Models: A Variational Inequality Approach. Springer-Verlag, Berlin-Heidelberg.
Colson, B., Marcotte, P., Savard, G., 2007. An overview of bilevel optimization. Ann. Oper. Res. 153 (1), 235–256. http://dx.doi.org/10.1007/s10479-007-0176-2.
Currie, G., Sarvi, M., Young, W., 2004. A new methodology for allocating road space for public transport priority. WIT Trans. Built Environ. 75 (2), 165–176. http://dx.doi.org/10.1007/s002540050446, URL: https://www.witpress.com/elibrary/wit-transactions-on-the-built-environment/75/12167.
Daganzo, C.F., 2007. Urban gridlock: Macroscopic modeling and mitigation approaches. Transp. Res. B 41 (1), 49–62. http://dx.doi.org/10.1016/j.trb.2006.03.001.
Daganzo, C.F., 2010. Structure of competitive transit networks. Transp. Res. B 44 (4), 434–446.
Daganzo, C.F., Geroliminis, N., 2008. An analytical approximation for the macroscopic fundamental diagram of urban traffic. Transp. Res. B 42, 771–781.
Dakic, I., Leclercq, L., Menendez, M., 2021. On the optimization of the bus network design: An analytical approach based on the three-dimensional macroscopic fundamental diagram. Transp. Res. B 149, 393–417. http://dx.doi.org/10.1016/j.trb.2021.04.012, URL: https://linkinghub.elsevier.com/retrieve/pii/S0191261521000758.
Dantsuji, T., Fukuda, D., Zheng, N., 2017. A macroscopic approach for optimizing road space allocation of bus lanes in multimodal urban networks through simulation analysis: An application to the tokyo CBD network. In: IEEE Conference on Intelligent Transportation Systems (ITSC). http://dx.doi.org/10.1109/ITSC.2017.8317936.
Dantsuji, T., Fukuda, D., Zheng, N., 2021. Simulation-based joint optimization framework for congestion mitigation in multimodal urban network: a macroscopic approach. Transportation 48 (2), 673–697. http://dx.doi.org/10.1007/s11116-019-10074-y.
de Palma, A., Lindsey, R., 2011. Traffic congestion pricing methodologies and technologies. Transp. Res. C 19 (6), 1377–1399. http://dx.doi.org/10.1016/j.trc.2011.02.010.
Edie, L., 1963. Discussion of traffic stream measurements and definitions. In: Almond, J. (Ed.), Proceedings of the 2nd International Symposium on the Theory of Traffic Flow. OECD, Paris, pp. 139–154.
Erath, A., Axhausen, K.W., 2010. Long Term Fuel Price Elasticity: Effects on Mobility Tool Ownership and Residential Location Choice. Swiss Federal Office of Energy (SFOE), Federal Office for the Environment (FOEN), Bern.
Farahani, R.Z., Miandoabchi, E., Szeto, W.Y., Rashidi, H., 2013. A review of urban transportation network design problems. European J. Oper. Res. 229 (2), 281–302. http://dx.doi.org/10.1016/j.ejor.2013.01.001.
Friesz, T.L., 1985. Transportation network equilibrium, design and aggregation: Key developments and research opportunities. Transp. Res. Part A: Policy Pract. 19 (5–6), 413–427.
Fu, H., Wang, Y., Tang, X., Zheng, N., Geroliminis, N., 2020. Empirical analysis of large-scale multimodal traffic with multi-sensor data. Transp. Res. C 118, 102725. http://dx.doi.org/10.1016/J.TRC.2020.102725.
GAMS Development Corporation, 2018. General algebraic modeling system (GAMS) release 25.1.
Geroliminis, N., Daganzo, C.F., 2008. Existence of urban-scale macroscopic fundamental diagrams: Some experimental findings. Transp. Res. B 42, 759–770.
Geroliminis, N., Levinson, D.M., 2009. Cordon pricing consistent with the physics of overcrowding. In: Lam, W.H.K., Wong, S.C., Lo, H.K. (Eds.), Transportation and Traffic Theory 2009: Golden Jubilee. Springer, pp. 219–240. http://dx.doi.org/10.1007/978-1-4419-0820-9_11.
Geroliminis, N., Zheng, N., Ampountolas, K., 2014. A three-dimensional macroscopic fundamental diagram for mixed bi-modal urban networks. Transp. Res. C 42, 168–181.
Gonzales, E.J., Daganzo, C.F., 2012. Morning commute with competing modes and distributed demand: User equilibrium, system optimum, and pricing. Transp. Res. B 46 (10), 1519–1534. http://dx.doi.org/10.1016/j.trb.2012.07.009.
Gonzales, E.J., Geroliminis, N., Cassidy, M.J., Daganzo, C.F., 2010. On the allocation of city space to multiple transport modes. Transp. Plan. Technol. 33 (8), 643–656. http://dx.doi.org/10.1080/03081060.2010.527171.
Guihaire, V., Hao, J.-K., 2008. Transit network design and scheduling: A global review. Transp. Res. Part A: Policy Pract. 42 (10), 1251–1273. http://dx.doi.org/10.1016/j.tra.2008.03.011.
Guler, S.I., Gayah, V.V., Menendez, M., 2016. Bus priority at signalized intersections with single-lane approaches: A novel pre-signal strategy. Transp. Res. C 63, 51–70. http://dx.doi.org/10.1016/j.trc.2015.12.005.
Guler, S.I., Menendez, M., 2014. Analytical formulation and empirical evaluation of pre-signals for bus priority. Transp. Res. B 64, 41–53. http://dx.doi.org/10.1016/j.trb.2014.03.004.
Haddad, J., Geroliminis, N., 2012. On the stability of traffic perimeter control in two-region urban cities. Transp. Res. B 46, 1159–1176.
Hansen, W.G., 1959. How accessibility shapes land use. J. Amer. Inst. Plan. 25, 73–76. http://dx.doi.org/10.1080/01944365908978307.
Holroyd, E., 1965. The optimum bus service: a theoretical model for a large uniform urban area. In: Vehicular Science, Proceedings of the 3rd International Symposium on the Theory of Traffic Flow. Elsevier, New York, New York, pp. 308–328.
Ibarra-Rojas, O.J., Delgado, F., Giesen, R., Muñoz, J.C., 2015. Planning, operation, and control of bus transport systems: A literature review. Transp. Res. B 77, 38–75. http://dx.doi.org/10.1016/j.trb.2015.03.002.
Ji, Y., Geroliminis, N., 2012. On the spatial partitioning of urban transportation networks. Transp. Res. B 46 (10), 1639–1656. http://dx.doi.org/10.1016/j.trb.2012.08.005.
Kepaptsoglou, K., Karlaftis, M., 2009. Transit route network design problem: Review. J. Transp. Eng. 135 (8), 491–505. http://dx.doi.org/10.1061/(ASCE)0733-947X(2009)135:8(491).
Kraus, M., 2012. Road pricing with optimal mass transit. J. Urban Econ. 72 (2–3), 81–86. http://dx.doi.org/10.1016/j.jue.2012.04.002.
Leclercq, L., Chiabaut, N., Trinquier, B., 2014. Macroscopic fundamental diagrams: A cross-comparison of estimation methods. Transp. Res. B 62, 1–12. http://dx.doi.org/10.1016/j.trb.2014.01.007.
Loder, A., Ambühl, L., Menendez, M., Axhausen, K.W., 2017. Empirics of multi-modal traffic networks – using the 3D macroscopic fundamental diagram. Transp. Res. C 82, 88–101. http://dx.doi.org/10.1016/j.trc.2017.06.009.
Loder, A., Ambühl, L., Menendez, M., Axhausen, K.W., 2019a. Understanding traffic capacity of urban networks. Sci. Rep. 9 (16283), http://dx.doi.org/10.1038/s41598-019-51539-5.
Loder, A., Axhausen, K.W., 2018. Mobility tools and use: Accessibility's role in Switzerland. J. Transp. Land Use 11 (1), 367–385. http://dx.doi.org/10.5198/jtlu.2018.1054.
Loder, A., Bressan, L., Wierbos, M.J., Becker, H., Emmonds, A., Obee, M., Knoop, V.L., Menendez, M., Axhausen, K.W., 2021. How many cars in the city are too many? Towards finding the optimal modal split for a multi-modal urban road network. Front. Future Transp. 2 (665006), http://dx.doi.org/10.3389/ffutr.2021.665006.
Loder, A., Dakic, I., Bressan, L., Ambühl, L., Bliemer, M., Menendez, M., Axhausen, K., 2019b. Capturing network properties with a functional form for the multi-modal macroscopic fundamental diagram. Transp. Res. B 129, 1–19. http://dx.doi.org/10.1016/j.trb.2019.09.004.

Luathep, P., Sumalee, A., Lam, W.H., Li, Z.-C., Lo, H.K., 2011. Global optimization method for mixed transportation network design problem: A mixed-integer linear programming approach. Transp. Res. B 45 (5), 808–827. http://dx.doi.org/10.1016/J.TRB.2011.02.002, URL: https://www.sciencedirect.com/science/article/pii/S0191261511000166.

Luo, Z.-Q., Pang, J.-S., Ralph, D., 1996. Mathematical Programs with Equilibrium Constraints. Cambridge University Press, Cambridge.

Magnanti, T.L., Wong, R.T., 1984. Network design and transportation planning: Models and algorithms. Transp. Sci. 18 (1), 1–55. http://dx.doi.org/10.1287/trsc.18.1.1.

Mariotte, G., Leclercq, L., Laval, J.A., 2017. Macroscopic urban dynamics: Analytical and numerical comparisons of existing models. Transp. Res. B 101, 245–267. http://dx.doi.org/10.1016/j.trb.2017.04.002.

Menendez, M., Daganzo, C.F., 2007. Effects of HOV lanes on freeway bottlenecks. Transp. Res. B 41 (8), 809–822. http://dx.doi.org/10.1016/J.TRB.2007.03.001, URL: https://www.sciencedirect.com/science/article/pii/S019126150700029X.

Miandoabchi, E., Farahani, R.Z., Dullaert, W., Szeto, W.Y., 2012. Hybrid evolutionary metaheuristics for concurrent multi-objective design of urban road and public transit networks. Netw. Spat. Econ. 12 (3), 441–480. http://dx.doi.org/10.1007/s11067-011-9163-x.

Migdalas, A., 1995. Bilevel programming in traffic planning: Models, methods and challenge. J. Global Optim. 7 (4), 381–405. http://dx.doi.org/10.1007/BF01099649.

Nagurney, A., 1993. Network Economics: A Variational Inequality Approach. Kluwer Academic Publishers, Boston.

Paipuri, M., Barmpounakis, E., Geroliminis, N., Leclercq, L., 2021. Empirical observations of multi-modal network-level models: Insights from the pNEUMA experiment. Transp. Res. C 131, 103300. http://dx.doi.org/10.1016/J.TRC.2021.103300.

Parry, I.W.H., 2009. Pricing urban congestion. Ann. Rev. Resour. Econ. 1 (1), 461–484. http://dx.doi.org/10.1146/annurev.resource.050708.144226.

Parry, I.W.H., Small, K.A., 2009. Should urban transit subsidies be reduced? Amer. Econ. Rev. 99 (3), 700–724. http://dx.doi.org/10.1257/aer.99.3.700.

Patz, A., 1925. Die richtige auswahl der verkehrslinien bei grossen strassenbahnnetzen. Verkehrstechnik 50/51, 977–983.

Pigou, A.C., 1920. the Economics of Welfare. Macmillan, London.

Rutherford, T.F., 1995. Extension of GAMS for complementarity problems arising in applied economic analysis. J. Econom. Dynam. Control 19 (8), 1299–1324. http://dx.doi.org/10.1016/0165-1889(94)00831-2.

Salzborn, F.J.M., 1972. Optimum bus scheduling. Transp. Sci. 6 (2), 137–148. http://dx.doi.org/10.1287/trsc.6.2.137.

Sarvi, M., Bagloee, S.A., Bliemer, M.C., 2016. Network design for road transit priority. In: Bliemer, M.C., Mulley, C., Moutou, C.J. (Eds.), Handbook on Transport and Urban Planning in the Developed World. Edward Elgar Publishing, Cheltenham, Northampton, pp. 355–374.

Schéele, S., 1980. A supply model for public transit services. Transp. Res. B 14 (1–2), 133–146.

Small, K.A., Verhoef, E.T., 2007. the Economics of Urban Transportation. Routledge, London, p. 276.

Smeed, R.J., 1968. Traffic studies and urban congestion. J. Transp. Econ. Policy 2, 33–70.

Sonntag, H., 1977. Linienplanung im öffentlichen Personennahverkehr (Ph.D. thesis). Technische Universität Berlin.

Statistisches Amt des Kantons Zürich, 2021. Regionalisierte Bevölkerungsprognosen für den Kanton Zürich. Zürich.

Sun, L., Tirachini, A., Axhausen, K.W., Erath, A., Lee, D.-H., 2014. Models of bus boarding and alighting dynamics. Transp. Res. Part A: Policy Pract. 69, 447–460. http://dx.doi.org/10.1016/j.tra.2014.09.007.

Swiss Federal Statistical Office and Swiss Federal Office for Spatial Development, 2017. Verkehrsverhalten der Bevölkerung- Ergebnisse des Mikrozensus Mobilität und Verkehr 2015. Bundesamt für Statistik BFS, Bundesamt für Raumentwicklung ARE, Neuchâtel.

Tilg, G., Ul Abedin, Z., Amini, S., Busch, F., 2020. Simulation-based design of urban bi-modal transport systems. Front. Future Transp. 1 (581622), http://dx.doi.org/10.3389/ffutr.2020.581622.

Tirachini, A., Hensher, D.A., 2012. Multimodal transport pricing: First best, second best and extensions to non-motorized transport. Transp. Rev. 32, 181–202. http://dx.doi.org/10.1080/01441647.2011.635318.

Tirachini, A., Hensher, D.A., Bliemer, M.C., 2014a. Accounting for travel time variability in the optimal pricing of cars and buses. Transportation 41 (5), 947–971. http://dx.doi.org/10.1007/s11116-014-9515-8.

Tirachini, A., Hensher, D.A., Rose, J.M., 2014b. Multimodal pricing and optimal design of urban public transport: The interplay between traffic congestion and bus crowding. Transp. Res. B 61, 33–54. http://dx.doi.org/10.1016/j.trb.2014.01.003.

van Nieuwkoop, R.H., 2014. Transportation Networks and Economic Equilibrium Modeling Issues and Applications (Ph.D. thesis). ETH Zürich, http://dx.doi.org/10.3929/ethz-b-000251651.

Vrtic, M., 2003. Simultanes Routen- und Verkehrsmittelwahlmodell (Ph.D. thesis). TU Dresden.

Wang, S., Meng, Q., Yang, H., 2013. Global optimization methods for the discrete network design problem. Transp. Res. B 50, 42–60. http://dx.doi.org/10.1016/J.TRB.2013.01.006, URL: https://www.sciencedirect.com/science/article/pii/S0191261513000179.

Yang, H., Bell, M.G.H., 1998. A capacity paradox in network design and how to avoid it. Trransp. Res. Part A: Policy Pract. 32 (7), 539–545.

Yildirimoglu, M., Geroliminis, N., 2014. Approximating dynamic equilibrium conditions with macroscopic fundamental diagrams. Transp. Res. B 70, 186–200. http://dx.doi.org/10.1016/j.trb.2014.09.002.

Yildirimoglu, M., Ramezani, M., Geroliminis, N., 2015. Equilibrium analysis and route guidance in large-scale networks with MFD dynamics. Transp. Res. C 59, 404–420. http://dx.doi.org/10.1016/j.trpro.2015.07.011.

Zheng, N., Dantsuji, T., Wang, P., Geroliminis, N., 2017. Macroscopic approach for optimizing road space allocation of bus lanes in multimodal urban networks through simulation analysis. Transp. Res. Rec. 2651, 42–51. http://dx.doi.org/10.3141/2651-05.

Zheng, N., Geroliminis, N., 2013. On the distribution of urban road space for multimodal congested networks. Transp. Res. B 57, 326–341. http://dx.doi.org/10.1016/j.sbspro.2013.05.009.

Zheng, N., Geroliminis, N., 2020. Area-based equitable pricing strategies for multimodal urban networks with heterogeneous users. Transp. Res. Part A: Policy Pract.ce 136, 357–374. http://dx.doi.org/10.1016/J.TRA.2020.04.009.

Zheng, N., Waraich, R.A., Geroliminis, N., Axhausen, K.W., 2012. A dynamic cordon pricing scheme combining a macroscopic and an agent-based traffic model. Transp. Res. Part A: Policy Pract. 46, 1291–1303. http://dx.doi.org/10.1016/j.tra.2012.05.006.